




# Clinically relevant mitochondrial-targeted therapy improves chronic outcomes after traumatic brain injury

W. Brad Hubbard,<sup>1,2,3,4</sup> Malinda L. Spry,<sup>1</sup> Jennifer L. Gooch,<sup>1</sup> Amber L. Cloud,<sup>5</sup> Hemendra J. Vekaria,<sup>1</sup> Shawn Burden,<sup>1</sup> David K. Powell,<sup>2</sup> Bruce A. Berkowitz,<sup>6</sup> Werner J. Geldenhuys,<sup>7</sup> Neil G. Harris<sup>8</sup> and  Patrick G. Sullivan<sup>1,2,4</sup>

Pioglitazone, an FDA-approved compound, has been shown to target the novel mitochondrial protein mitoNEET and produce short-term neuroprotection and functional benefits following traumatic brain injury.

To expand on these findings, we now investigate the dose- and time-dependent effects of pioglitazone administration on mitochondrial function after experimental traumatic brain injury. We then hypothesize that optimal pioglitazone dosing will lead to ongoing neuroprotection and cognitive benefits that are dependent on pioglitazone-mitoNEET signalling pathways. We show that delayed intervention is significantly more effective than early intervention at improving acute mitochondrial bioenergetics in the brain after traumatic brain injury. In corroboration, we demonstrate that mitoNEET is more heavily expressed, especially near the cortical contusion, in the 18 h following traumatic brain injury. To explore whether these findings relate to ongoing pathological and behavioural outcomes, mice received controlled cortical impact followed by initiation of pioglitazone treatment at either 3 or 18 h post-injury. Mice with treatment initiation at 18 h post-injury exhibited significantly improved behaviour and tissue sparing compared to mice with pioglitazone initiated at 3 h post-injury. Further using mitoNEET knockout mice, we show that this therapeutic effect is dependent on mitoNEET. Finally, we demonstrate that delayed pioglitazone treatment improves serial motor and cognitive performance in conjunction with attenuated brain atrophy after traumatic brain injury.

This study illustrates that mitoNEET is the critical target for delayed pioglitazone intervention after traumatic brain injury, mitochondrial-targeting is highly time-dependent after injury and there is an extended therapeutic window to effectively treat mitochondrial dysfunction after brain injury.

1 Spinal Cord and Brain Injury Research Center, University of Kentucky, Lexington, KY 40536, USA

2 Department of Neuroscience, University of Kentucky, Lexington, KY 40508, USA

3 Department of Physiology, University of Kentucky, Lexington, KY 40508, USA

4 Lexington VA Healthcare System, Lexington, KY 40502, USA

5 College of Medicine, University of Kentucky, Lexington, KY 40508, USA

6 Department of Ophthalmology, Visual and Anatomical Sciences, Wayne State University School of Medicine, Detroit, MI 48202, USA

7 Department of Pharmaceutical Sciences, School of Pharmacy, West Virginia University, Morgantown, WV 26506, USA

8 UCLA Brain Injury Research Center, Department of Neurosurgery, and Intellectual Development and Disabilities Research Center, David Geffen School of Medicine, University of California at Los Angeles, Los Angeles, CA 90095, USA

Correspondence to: Patrick G. Sullivan, PhD  
Spinal Cord and Brain Injury Research Center, University of Kentucky  
475 Biomedical & Biological Sciences Research Building  
741 South Limestone St Lexington, KY 40536-0509, USA  
E-mail: patsullivan@uky.edu

**Keywords:** controlled cortical impact; mitochondria; Seahorse; synapse; MRI

**Abbreviations:** CCI = controlled cortical impact; HNE = 4-hydroxy-2-nonenal; MWM = Morris water maze; NOR = novel object recognition; NSS = neurological severity score; OCR = oxygen consumption rate; PPAR = peroxisome proliferator-activated receptor; RI = recognition index; TBI = traumatic brain injury

## Introduction

Traumatic brain injury (TBI) continues to have a devastating impact on affected individuals and economic burden. Current reports suggest that over 4 million people are living with a TBI-related disability in the USA.<sup>1</sup> The number of TBI-related disabilities are growing and there continues to be a lack of treatment options to mitigate neurological consequences. To date, preclinical and clinical studies have been focused on targeting secondary injury processes to slow the progression of injury pathology, thereby reducing cellular stress on neurons and glia. Mitochondrial dysfunction is a major secondary injury cascade that occurs after head impact and has been shown to be an important process to target for neuroprotection and behavioural improvement.<sup>2–8</sup> Indeed, our group has shown that mitochondrial-directed pharmaceuticals that modulate reactive oxygen species production, mitochondrial membrane potential, mitochondrial dynamics and mitochondrial-driven apoptosis confer efficacy in neurobehavioural outcomes.<sup>2–6,9,10</sup> Importantly, our previous research has shown that pioglitazone is one such pharmaceutical that improves mitochondrial bioenergetics, provides neuroprotection and promotes cognitive recovery.<sup>11,12</sup>

Pioglitazone is a thiazolidinedione and a ligand for peroxisome proliferator-activated receptors (PPARs).<sup>13</sup> Specifically, PPAR- $\gamma$  has a well-established role in the regulation of gene expression for processes such as glucose homeostasis, cellular differentiation and apoptosis.<sup>14</sup> Past studies have focused on PPAR- $\gamma$  as a target for modulation of neuroinflammation, via decreased production of proinflammatory mediators in microglia and macrophages, resulting from neurological injury.<sup>15</sup> However, recent reports highlight that neuroprotection imparted by PPAR- $\gamma$  agonists could be due to a number of transcriptional changes, including decreased oxidative stress, enhanced neurogenesis and vasoreactivity in addition to inflammatory modulation.<sup>16,17</sup>

With reports from various groups demonstrating that pioglitazone can improve cortical sparing after CNS injury, it was important to determine the mechanism of action.<sup>12,18</sup> It was hypothesized that the modulation of inflammation through PPAR- $\gamma$  was the primary mechanism for neuroprotection, however, pharmacological PPAR- $\gamma$  inhibition did not prevent neuroprotection.<sup>18</sup> Further, our past research shows that pioglitazone is required to be pharmacokinetically active to exert significantly increased mitochondrial function<sup>12</sup> and exerts its effects on mitochondrial bioenergetics in a fast-acting manner that would not be dependent on transcriptional changes.<sup>11</sup> These past findings point to a unique therapeutic mechanism for pioglitazone following TBI, independent of PPAR- $\gamma$  signalling.

Pioglitazone has a high binding affinity for a specific mitochondrial membrane protein, mitoNEET, and results in a stabilization of its conformational structure.<sup>19,20</sup> The exact biological and

pathological consequences of mitoNEET binding are unclear, although our past research does show that it promotes mitochondrial respiration in both TBI and spinal cord injury.<sup>11,21</sup> Overexpression of mitoNEET, and therefore binding potential, in white adipose tissue can lead to uncoupling of oxidative phosphorylation, lowering mitochondrial membrane potential and reactive oxygen species reduction.<sup>22</sup> It was also found that mitoNEET plays a distinct role in redox-sensing, governed by iron–sulphur cluster transfer, which enables it to regulate mitochondrial function.<sup>23</sup> Our group has shown that mitoNEET is the prevailing therapeutic target of pioglitazone following TBI.<sup>11</sup>

To understand the pharmacodynamics of pioglitazone following TBI, we have systemically examined dose- and time-dependent mitochondrial responses based on pioglitazone treatment. As the therapeutic effect of pioglitazone is not dependent on transcriptional changes after TBI, it is quite possible that therapeutic effects can still be achieved with delayed treatment. In this study, we sought to examine the therapeutic window of pioglitazone by initiating therapy at various time points after injury based on the primary outcome of mitochondrial bioenergetics in the hippocampus. Furthermore, it is crucial to examine the therapeutic window of opportunity to determine appropriate temporal targeting based on pathological processes after TBI. We hypothesize that the optimal dosing paradigm defined by improvement in mitochondrial function will result in better neuroprotection and behaviour improvement.

To examine preclinical efficacy, we used the optimal dosing regimen following TBI to examine the therapeutic effects on neurobehavioural outcomes, including neurological severity score (NSS), novel object recognition (NOR) and the Morris water maze (MWM). Further, we assessed neuroprotection via two independent measures, *in vivo* T<sub>2</sub> MRI and Nissl-stained post-mortem coronal tissues. We show that behavioural improvements imparted by pioglitazone are dependent on the presence of mitoNEET. Finally, we perform a long-term longitudinal study examining brain atrophy and cognitive ability over time following delayed pioglitazone administration.

## Materials and methods

### Animals

All of the studies performed were approved by the University of Kentucky Institutional Animal Care and Usage Committee and the United States Veterans Affairs Animal Component of Research Protocol. Additionally, the Division of Laboratory Animal Resources at the University is accredited by the Association for the Assessment and Accreditation for Laboratory Animal Care, International (AAALAC, International) and all experiments were

performed with its guidelines. All animal experiments were compliant with ARRIVE guidelines and experiments were carried out in accordance with the National Institutes of Health Guide for the Care and Use of Laboratory Animals (NIH Publications No. 8023, revised 1978). All experiments were conducted using male and female adult (2–3 months) wild-type C57BL/6 (Jackson Laboratories) or male and female mitoNEET null mice with an average mass of 25 g. Using mitoNEET null mice at 2 to 3 months of age for injury and subsequent cognitive assessment is critical as our group has previously shown that male mitoNEET null mice at 6 months of age display motor deficits.<sup>24</sup> mitoNEET null mice were gifted to the laboratory and the generation of the model was previously described.<sup>11,25</sup>

Animals were randomly assigned to groups, using random number generators. Researchers were blinded to treatment groups during outcome assessment and data analysis. The animals were housed five per cage and maintained in a 14-h light/10-h dark cycle. Confounding factors were minimized by including various treatment groups in the same cage, ensuring all experimental groups are operated on and analysed at the same time (especially if the assay required multiple cohorts of animals), and all animals were housed in the same room. All animals were fed a balanced diet *ad libitum* and water was reverse osmosis generated. All mitochondrial experiments were performed with technical triplicates. The exact numbers of animals used in each study are reported in the figure legends.

### Experimental design and drug administration

To determine the optimal dose of pioglitazone following TBI, mice received a bolus (intraperitoneal, i.p.) administration of pioglitazone (100 µl volume; 1:1 DMSO and PEG400) or vehicle at 15 min after severe controlled cortical impact (CCI) followed by subcutaneous implantation of osmotic mini-pump tuned to deliver either 1, 10, 20 or 40 mg/kg/day pioglitazone or vehicle, equivalent to initial bolus. Our studies used either a 3-day duration Alzet Mini Pump 1003D (release of 1 µl/h) or 7-day duration Alzet Mini Pump 1007D (release of 0.5 µl/h) for the 48 h mitochondrial studies and the neuroprotection studies, respectively. To then determine the therapeutic window of opportunity for the optimized dose of pioglitazone, mice received a bolus (i.p.) administration of pioglitazone at either 1, 3, 6, 12, 18 or 24 h after severe CCI followed by implantation of osmotic mini-pump at the optimized dose. Booster injections were given at 24 and 47 h post-injury. Total mitochondrial bioenergetic measures, obtained at either 24 or 48 h post-injury, were the primary end point of these studies. To determine mitoNEET expression following TBI, mice were subjected to severe CCI and euthanized at 1, 3, 6, 12, 18 and 24 h post-injury. To further evaluate ongoing synaptic mitochondrial health in the ipsilateral cortex, mice received a bolus (i.p.) administration of pioglitazone at 18 h after severe CCI followed by implantation of osmotic mini-pump tuned to deliver 20 mg/kg/day pioglitazone. Fresh ipsilateral cortical tissue was harvested in two separate cohorts at 48 h and 7 days post-injury. Synaptic and non-synaptic subpopulations of mitochondria were examined.

Detailed timelines of all behavioural experiments can be found in [Supplementary Fig. 1](#). To evaluate the neuroprotective and behavioural effects of pioglitazone, a 20 mg/kg bolus (i.p.) injection was given at either 3 or 18 h post-injury after severe CCI followed by implantation of osmotic mini-pump (20 mg/kg/day pioglitazone or vehicle). Additional bolus injections were given every 24 h until 7 days post-injury. Subacute behavioural assays were conducted between 8 and 9 days (NOR) and between 12 and 16 days post-injury (MWM). Brain tissue was harvested at 21 days post-injury. To assess whether targeting of mitoNEET is crucial for cognitive

improvement and neuroprotection, a 20 mg/kg bolus (i.p.) injection was given at 18 h post-injury to both C57BL/6 and mitoNEET null mice after severe CCI followed by pioglitazone administration as performed previously. Mice were given behavioural tasks, NOR at 3 days post-injury and MWM at 7–11 days post-injury and brains were harvested at 14 days post-injury. Long-term behavioural assays were performed to assess the lasting motor and cognitive effects of TBI and subsequent pioglitazone administration. In this cohort, mice performed acute motor function assay, which consisted of beam-walking tasks that compromised the NSS; this was assayed at 1, 3 and 7 days post-injury. Further, this cohort performed NOR at 40, 70, 95, 125 and 150 days post-injury along with MWM at 10–15, 85–90 and 160–165 days post-injury. Although serial behavioural testing was conducted in the chronic cohort of animals, adequate rest time was given to animals between tasks. Total animal numbers can be found in [Supplementary Table 1](#).

### Controlled cortical impact

All surgical procedures were performed as previously described and were classified as severe (1.0 mm depth of contusion at 3.5 m/s with dwell time of 500 ms).<sup>6</sup> Before injury, animals were anaesthetized (2–5% isoflurane) and their heads were shaved and cleaned. Mice were placed in a Kopf stereotaxic frame for proper positioning under a pneumatic impactor (Precision Science Instruments) with body temperature maintained at 37°C using an isothermal pad. A 4-mm craniotomy was performed lateral to the central fissure on the left side of the skull centred between lambda and bregma, without disrupting the dura. Injury groups then received a unilateral injury directly to the surface of the brain using a 3 mm flat-tip impactor. Sham animals received a craniotomy but did not receive an impact to the brain. Following the injury, the craniotomy was covered with a sterilized plastic surgical disc and incisions were closed with surgical staples. Both sham and injured mice were removed from isoflurane exposure (total duration of 10–12 min) and the stereotaxic frame. They were placed in a clean, temperature-controlled cage until the animals were mobile and fully responsive.

### Total mitochondrial isolation

Mitochondria were isolated using previously employed differential mitochondrial isolation methods.<sup>26</sup> Animals were asphyxiated with CO<sub>2</sub> and rapidly decapitated. Following decapitation, the brain was rapidly removed, rinsed in ice-cold mitochondrial isolation buffer (IB; 215 mM mannitol, 75 mM sucrose, 0.1% BSA, 1 mM EGTA and 20 mM HEPES at pH 7.2), and dissected on ice. Brain tissue samples from ipsilateral cortex (no. 2 punch, 4-mm diameter tissue punch centred on cortical impact site), ipsilateral hippocampus and limbic regions were homogenized using 8–10 strokes in Dounce homogenizers; the homogenate was placed in a 2-ml microfuge tube and then centrifuged at 1300g for 3 min. The supernatant was placed in a fresh tube and the pellet was resuspended in IB to be spun again at 1300g for 3 min. The supernatants from the first and second spins were collected in separate tubes and spun at 13000g for 10 min. The pellets from both tubes were combined, resuspended in 500 µl of IB and placed in a nitrogen cell disruptor (Parr Instrument Company) at 1200 psi for 10 min to release trapped mitochondria within synaptosomes. The pressure in the nitrogen cell disruptor was rapidly released after 10 min. The resulting total mitochondrial suspensions were transferred to 1.5-ml centrifuge tubes and topped with IB and centrifuged at 10000g for 10 min. The pellets were resuspended in IB (without EGTA) to bring the approximate protein concentration to 10 mg/ml. Protein concentration was determined using BCA protein assay kit (Pierce,

Cat No 23,227) recording the absorbance at 560nm on a Biotek Synergy HT plate reader.

### Synaptic mitochondrial isolation

For a detailed breakdown of the fractionated mitochondrial magnetic separation technique, see Hubbard *et al.*<sup>27</sup> Briefly, ipsilateral cortical tissue was removed as previously described, homogenized and then centrifuged at 1300g for 3 min. This homogenate contains free-floating mitochondria, derived from glia, endothelial cells and neuronal soma, as well as intact synaptosomes, vesicles that form and contains mitochondria from the neuronal synapse. The supernatant was placed in a fresh tube and the pellet was resuspended in IB to be spun again at 1300g for 3 min. The supernatants from the first and second spins were incubated with anti-Tom22 microbeads (Miltenyi Biotec) at a concentration of 4  $\mu$ l for every 1 mg of starting wet tissue weight for 30 min. The mixture was then added to MACS separation LS columns, attached to Quadro MACS Separator (Miltenyi Biotec, Cat No 130-097-040), to capture free mitochondria (non-synaptic fraction). The eluate, containing synaptosomes, was collected for subsequent use. The columns were plunged causing magnetically attached mitochondria to dissociate and enter into the 15-ml conical tube. The sample was transferred to 1.5 microcentrifuge tube and centrifuged at 13000g for 10 min at 4°C. Meanwhile, the eluate from the LS columns, which contains synaptosomes, was spun at 13000g for 10 min before being placed into the pressurized nitrogen cell disruptor. Once the synaptosomes were burst, the resulting solution was incubated with anti-Tom22 microbeads (1  $\mu$ l for every 1 mg of starting tissue) for 30 min. All sequential steps were performed as previously described.

### Measurement of mitochondrial bioenergetics

Measurements of mitochondrial bioenergetics in isolated mitochondria were completed using either Seahorse XFe24 or Seahorse XFe96 Flux Analyzer (Agilent Technologies) as published previously using slight modifications.<sup>10</sup> The oxygen consumption rates (OCRs) were measured in the presence of mitochondrial substrates, inhibitors and uncouplers of the electron transport chain using previously described methods. On the day before the assay, the sensor cartridge of Extracellular Flux kit was hydrated according to the manufacturer's instructions. The day of the assay injection ports A to D of the sensor cartridge were loaded separately or in combinations of substrates/inhibitors/uncouplers to measure different states of respiration. Before loading, the stocks were diluted appropriately in respiration buffer (RB; 125 mM KCl, 0.1% BSA, 20 mM HEPES, 2 mM MgCl<sub>2</sub> and 2.5 mM KH<sub>2</sub>PO<sub>4</sub>, adjusted to pH 7.2) such that after each sequential injection the final concentration of the modulators were 5 mM pyruvate, 2.5 mM malate and 1 mM ADP (via Port A), 2.5  $\mu$ M oligomycin A (via Port B), 4  $\mu$ M FCCP (via Port C) and 1  $\mu$ M rotenone and 10 mM of succinate (via Port D). For the XFe24 analyser, 10  $\mu$ g total mitochondrial protein were loaded per well in a volume of 50  $\mu$ l. For the XFe96 analyser, 6  $\mu$ g total mitochondria, 3  $\mu$ g non-synaptic and 6  $\mu$ g synaptic mitochondrial protein were loaded per well in a volume of 30  $\mu$ l. The assay plates were centrifuged at 3000 rpm for 4 min at 4°C. Additional respiration buffer was added to bring the starting volume to 475  $\mu$ l or 175  $\mu$ l for the XFe24 and XFe96, respectively. After calibration step, the utility plate was replaced by the assay plate carrying mitochondria. The assays were carried out under previously optimized conditions. OCRs were measured for states of mitochondrial respiration. State III<sub>C1</sub> response in presence of 5 mM pyruvate, 2.5 mM malate and 1 mM ADP (Port A) was measured followed by State IV response in presence of 2.5  $\mu$ M oligomycin A (Port B).

Sequentially, State V<sub>C1</sub> and State V<sub>C2</sub> OCR rates were recorded automatically in presence of 4  $\mu$ M FCCP (Port C); 0.1  $\mu$ M rotenone and 10 mM of succinate (Port D), respectively. Raw OCR values were used for analysis within a given experiment and reported in all figures. Plate-to-plate and day-to-day variation may result in variable absolute OCR values between experiments, necessitating the use of blocking factor in statistical analysis.

### Histopathological analysis

Cohorts of mice from the long-term studies were euthanized by intraperitoneal injection of Fatal Plus (Vortech Pharmaceuticals) before transcardial perfusion with cold, sterile saline followed by either cold 4% paraformaldehyde (PFA) or 10% buffered formalin. After perfusion, mice were decapitated and the brains were then removed from the skull and post-fixed in 4% PFA for 24 h. Following post-fixation, tissue was placed into 1:1 4% PFA/30% sucrose mixture followed by 30% sucrose PBS buffer solution for at least 48 h for cryoprotection. The brain tissue was cut into 35- $\mu$ m thick coronal sections using a freezing stage, sliding microtome. A series of coronal tissue sections spaced  $\sim$ 400  $\mu$ m apart were mounted on slides, stained with cresyl violet and subjected to image analysis for assessment of cortical tissue sparing. Quantitative assessment of cortical damage employed a blinded unbiased tracing protocol to compare ipsilateral cortex to contralateral cortex. All slides were assessed blindly with respect to treatment group, for region of interest analysis to measure cortical sparing, using ImageJ software (NIH, USA) or HALO quantitative tissue analysis software (Indica Labs; Albuquerque, NM, USA). Data were converted to percentage of the contralateral cortex, which served as an internal control for each animal.

To examine mitoNEET expression, another series of coronal sections was used for immunohistochemistry. Tissues were blocked with 5% normal goat serum in 0.1% Triton X-100/1  $\times$  TBS before incubation in rabbit anti-mitoNEET antibody (Abcam, no. ab203096) overnight at 4°C. On the following day, tissue sections were rinsed and incubated in goat anti-rabbit IgG H&L (HRP) (Abcam, no. ab205718) for 1 h. The tissue was washed before incubating in Avidin-Biotin complex (Vector Laboratories) for 1 h and then treating with 3,3'-diaminobenzidine as directed by the manufacturer (Vector Laboratories). After washing, sections were mounted on slides, dried overnight and coverslipped. Slides were scanned on the Zeiss Axio Scan Z.1 and whole brain, ipsilateral cortex and ipsilateral hippocampus were all traced to define regions of interest in HALO. Images were quantified using area quantification with consistent parameters to identify stain colour and thresholds for stain intensity.

### Adjusted neurological severity score

Mice were tested at 1, 3 and 7 days post-injury for functional motor recovery. The adjusted NSS (aNSS) is based on 14-point test measures coordinated motor function and balance as a measurement of motor function/recovery following injury.<sup>11</sup> This score is based on the functional ability measured during the beam-walk test. The day before injury, all animals were trained to traverse elevated beams of 3, 2, 1 and 0.5 cm in width and a 0.5 cm diameter rod. At 24, 72 and 120 h post-injury, mice were allowed to traverse the beams and scored as follows. The four largest beams had a maximum score of 3 points and the smallest 0.5-cm diameter rod had a maximum score of 2 points. For the largest four beams, 1 point was deducted if the animal had one or more footfalls or became inverted during the test. For the 0.5-cm rod, 1 point was deducted for inversion on the rod. For all beams or rods, if an animal was



unwilling to traverse the beam or fell off during the test, the animal received a score of zero for that beam.

### Novel object recognition test

The NOR test was performed according to published protocols for rodents with small modifications.<sup>2</sup> The interaction with objects was either hand scored (3 h versus 18 h dosing efficacy study) or analysed by the behavioural tracking software Ethovision XT (Noldus, Leesburg, VA, USA) for proximity of the nose point to the objects (mitoNEET knockout study and long-term efficacy study). Comparative analysis was conducted to show the data is comparable between the two methods (data not shown). All behavioural testing was conducted during morning hours. Mice were acclimated 2 days following injury to either a 10.5 × 19 × 8-inch or 16 × 16 × 12-inch well-lit box for 1 h. At the time of assessment (see 'Experimental design and drug administration' section), mice were placed back into their individual testing box and allowed to explore two identical objects placed in opposite corners for 5 min (days post-injury specified in each experiment). To be included in behaviour analyses, animals had to have a total exploration time of 10 s with the objects in the T1 phase of the NOR test and exhibit uninhibited movement. Mice were excluded if they showed a marked preference for one familiar object over another familiar object (>80% of total exploration time). One day later, mice were placed back into their testing cage for 5 min with one of the previously explored objects and a novel object. The amount of time spent exploring each object was recorded. Again, the experimenter ensured a total object exploration time of at least 10 s for each animal by giving an additional minute of exploration time if needed. The recognition index (RI) was calculated by: [(time spent with novel object) / (time with novel object + time with familiar object) × 100].

### Morris water maze

A variant of the MWM task was used to assess cognitive function/dysfunction following TBI in these experiments.<sup>10</sup> All behavioural testing was conducted during morning hours. The maze was in low light and consisted of a circular pool filled with water (27°C). A clear Plexiglass platform 13 cm in diameter was laid 0.5–1.0 cm below the surface rendering it invisible and was used as the goal platform. The pool was situated in a room that had numerous extra-maze cues that remained constant throughout the experiment. A video camera system was placed directly above the centre of the pool recorded swimming performance and each video recorded was processed by a video motion analyser (Ethovision XT, Noldus). Water maze testing was performed at previously specified time points (Supplementary Fig. 1) and training consisted of four daily trials, one each starting from a different labelled quadrant. Each trial was initiated by placing the mouse into the water in a quadrant either adjacent or opposite to the platform. The platform location was fixed throughout the training. Each trial lasted 60 s or until the mouse located the platform. Mice that did not find the platform were guided to it and given a latency score of 60 s. Each mouse was required to spend 15 s on the platform at the end of each trial. During this learning period, mice used external visual cues as a reference to find the submerged platform. The latency to find the platform was recorded for each trial. On the fifth day, mice were given one probe trial in which the platform was removed. The first dependent measure was the number of times the mouse crossed over the platform arena. A second dependent measure was the time spent swimming in each quadrant.

### MRI

MRI was conducted using an approach similar to our previously published work.<sup>11</sup> In summary, a 7 T Bruker/Siemens Clinscan MRI

scanner was used to image mouse brains at 19–20 days post-injury following pioglitazone treatment in the subacute study. For the longitudinal study, MRIs were completed prior to injury (–7 days), 30, 100 and 166 days post-injury; these time points were chosen based on previous research.<sup>28</sup> During the imaging, animals were placed under continuous isoflurane anaesthesia, which was introduced through a nose cone, and the animal's head was placed under the head coil. Temperature was controlled with a hot bath warmed body cradle. Temperature and respiration were monitored using SA Instruments hardware and software. After inserting the animal and coil into the MRI scanner, localizers in the three orthogonal planes were used to focus and homogenize the magnetic field around the injured brain tissue. Following localization, T<sub>2</sub>-weighted images were acquired with a turbo spin echo sequence using prescan normalization to compensate for surface coil inhomogeneity in the coronal plane yielding 12 subsequent slices centred around the injury site with a field of view of 40 × 40 × 0.7 mm with a pixel resolution of 384 × 512. The imaging parameters were: echo time = 42 ms, repetition time = 2070 ms, prescan normalization to remove coil spatial inhomogeneities, phase encoding direction set to anterior-posterior and a total acquisition time of 11.25 min. MRI images were generated using Syngo Medical Imaging software (Siemens AG, Germany). Quantification of these images were conducted in a similar manner to those reported previously.<sup>11</sup> In summary, all images were processed with brain extraction tool (BET) and then analysed with Mango (open licence, UT Southwestern). For each of the 12 coronal images, the mean and standard deviation (SD) of the signal intensity of the whole brain (including the injury) were calculated. A threshold was then applied for each brain where any voxel >3 SD above the total mean signal was considered T<sub>2</sub> hyperintense 'injured tissue'. The T<sub>2</sub>-weighted cortical sparing was then calculated by the total volume of tissue on the injured hemisphere minus the T<sub>2</sub> hyperintense voxels on the injured hemisphere divided by the total volume of tissue on the contralateral hemisphere minus T<sub>2</sub> hyperintense voxels.

### Tensor-based deformation analysis

All T<sub>2</sub> were converted to nifti image format and the header dimensions were expanded by ×10 to enable brain extraction from extracranial tissue using the FSL BET.<sup>29</sup> All data were used to construct study-specific, mean deformation template (MDT) images using the antsMultivariateTemplateConstruction script<sup>30</sup> from Advanced Normalization Tools (ANTs, v.2.3.3)<sup>31</sup> that consisted of bias field correction and a three-stage coregistration procedure of rigid, affine and non-linear deformable registrations. Two MDT templates were created to reduce the impact of age on the group-related effects; preinjury and 30 days post-injury data from all groups were used to compute the first template, and post-injury data from 100 and 166 days groups were used to create the second template. The raw data from the two age-matched groups were then separately coregistered to their respective MDT templates using a two-stage affine and symmetric diffeomorphic registration under ANTs, but this time initiated from a subject-to-template-space affine transformation calculated using the FSL tool FLIRT.<sup>32,33</sup> The resulting deformation field was then used to derive the Jacobian determinant that provides an indication of the local tissue expansion compared to the age-matched MDT (referred herein as tissue swelling), or the local tissue compression (referred herein as tissue atrophy). All data were masked for a common space to ensure a contribution from all mice to each voxel, following which voxel-based Jacobian values from sham group data were used to calculate z-scores per voxel either side of the sham data, for each injured mouse. The number of voxels surviving a z

thresholded of 2.33 ( $P < 0.01$ ) were summed over each mouse brain and converted to a volume for statistical testing.

## Molecular modelling

Molecular modelling of pioglitazone interacting with mitoNEET was performed using the MOE 2020.09 software package. The protein crystal structure PDB 6DE9<sup>34</sup> was obtained from the Protein Data Bank and prepared for docking using the QuickPrep module. Missing hydrogens were added and the pH of the system set at 7.4. The SiteFinder module allowed for the detection of the binding pocket close to previous indicated Trp/Phe interacting residues by NMR studies.<sup>19</sup> Induced-fit docking procedure was used and the top pose with the highest (most negative) binding energy further evaluated.

## Statistical analysis

Power analysis was conducted (using G\*Power statistical software, v.3.0.10) for all experimental data and based on previous published literature from our group.<sup>2,10</sup> Analysis was completed based on the ANOVA statistical tests and output of *F*-score. *A priori* analysis was performed and effect size was calculated based on expected mean SD within each group, which varied based on outcome measure. For example, sample size was calculated for behavioural experiments using the following parameters:  $\alpha = 0.05$ ,  $1 - \beta = 0.8$  and standard deviation 20% of mean (effect size of 1.12) for experimental groups. Primary outcomes for sample size determination were hippocampal mitochondrial function and probe trial target arena time (cognitive behavioural outcomes). Some experiments included both male and female mice (Supplementary Table 1), although were not powered to detect for sex differences. Based on deviation and detectable differences, it was determined that only a subset of the mitochondrial aliquots was needed to measure oxidative damage markers.

Statistical analysis was performed using Graph Pad Prism (GraphPad Software, CA, USA) or JMP 12 (SAS, NC, USA). For all analyses, a significant difference among groups was defined as  $P < 0.05$ . For each measure, data were measured using interval/ratio scales. The Brown-Forsythe and Bartlett's tests were performed to ensure homogeneity of variance. Furthermore, the Shapiro-Wilk test was completed to ensure normality. As these criteria were met for all experimental data, parametric statistics were employed for all analyses, except for NSS paradigm (see next paragraph). For mitochondrial data, raw OCR values were used for analysis within a given experiment. For therapeutic window analysis, no difference was detected between shams administered vehicle or sham, so these groups were combined and represent dotted baseline. Plate-to-plate and day-to-day variation may result in different absolute OCR values between experiments. As such, we used a randomized block design with a blocking factor of assay day (i.e. different Seahorse plates) when performing the one-way ANOVA. Statistical outliers, after averaging technical triplicates, were identified by internally studentized residuals as previously published<sup>2,26</sup>; details of any outlier identification are provided in Supplementary material. For mitochondrial respiration analysis, one-way ANOVA was performed with all means compared to vehicle-treated CCI groups followed by Dunnett's *post hoc* test, where appropriate. For one-way ANOVA tests where all means were compared to each other, the Tukey's *post hoc* test was used, where appropriate.

For behavioural outcomes, one-way or repeated measures two-way ANOVA was performed to compare the effects of treatment and vehicle on dependent measures from MWM and NOR. Since the NSS assay is based on a scale of 0–14, non-parametric

Kruskal-Wallis test was performed, with Dunn's *post hoc*. The datasets were evaluated using an ANOVA, and when appropriate, *post hoc* comparisons employing the Tukey's test or Dunnett's test, depending on group comparisons. For the long-term behavioural study, RI scores were compared to chance performance (50%) using a one-sample *t*-test to ensure memory function.

## Data availability

The derived data that support the findings of this study are available from the corresponding author, on reasonable request.

## Results

### Dose optimization of pioglitazone following controlled cortical impact

As pioglitazone is known to interact with mitoNEET (see molecular model; Fig. 1A), we focused our initial studies on the effect pioglitazone has on acute mitochondrial bioenergetics in the injured brain. Recent studies have shown that post-injury treatment with pioglitazone is able to attenuate mitochondrial dysfunction.<sup>11,12</sup> Previously, we demonstrated that lower doses of pioglitazone were more effective at rescuing mitochondrial bioenergetics *ex vivo* after calcium insult.<sup>11</sup> Further, we determined that 10 mg/kg pioglitazone imparted greater bioenergetic restoration *in vivo* following CCI compared to 1 mg/kg pioglitazone. Although, so far, no rigorous dose-response curve has been generated for pioglitazone following CCI. In corroboration of our previous results,<sup>11</sup> we found that 10 mg/kg-treated mice increased State  $V_{C1}$  respiration compared to vehicle CCI groups. However, we show that 20 mg/kg pioglitazone is most effective at restoring bioenergetics at 24 h following CCI and is significantly higher compared to vehicle CCI group (Fig. 1B). As such, 20 mg/kg/day pioglitazone was used for each subsequent study in this paper.

### Therapeutic window of opportunity of pioglitazone after controlled cortical impact

The importance of defining the window for preclinical therapeutics cannot be overstated in terms of translational potential. Our group has previously shown that mitochondrial-targeted drugs, such as mitochondrial uncoupling agents and cyclosporin A, are promising candidates for TBI treatment that have extended therapeutic windows after injury.<sup>6,35</sup> Further, there is a need to identify drugs that have long therapeutic windows (>4 h after injury) for treatment of clinical TBI.<sup>36,37</sup> To examine the therapeutic window for pioglitazone, we conducted rigorous experimentation consisting of delayed initiation of 20 mg/kg pioglitazone treatment ranging from 1 to 24 h after CCI. The primary end point for these studies was State  $III_{C1}$ -driven mitochondrial respiration in mitochondria from ipsilateral hippocampus, although regional evaluation also focused on ipsilateral cortex and the limbic region. The ipsilateral hippocampus was chosen for its proximity to the injury, vulnerability to secondary damage, its major role in cognitive function and relevance to the memory and learning assays conducted in later experiments. Previous studies from our laboratory showed that pioglitazone administration delayed to 12 h post-injury could rescue mitochondrial respiration at 13 h post-injury, demonstrating the first evidence of an extended therapeutic window.<sup>11</sup> For mitochondria from the ipsilateral cortex, there were no beneficial effects on mitochondrial respiration when pioglitazone treatment was initiated at either 1 or 3 h post-injury compared to vehicle treatment (Fig. 1C). However, there was a significant increase in multiple states of

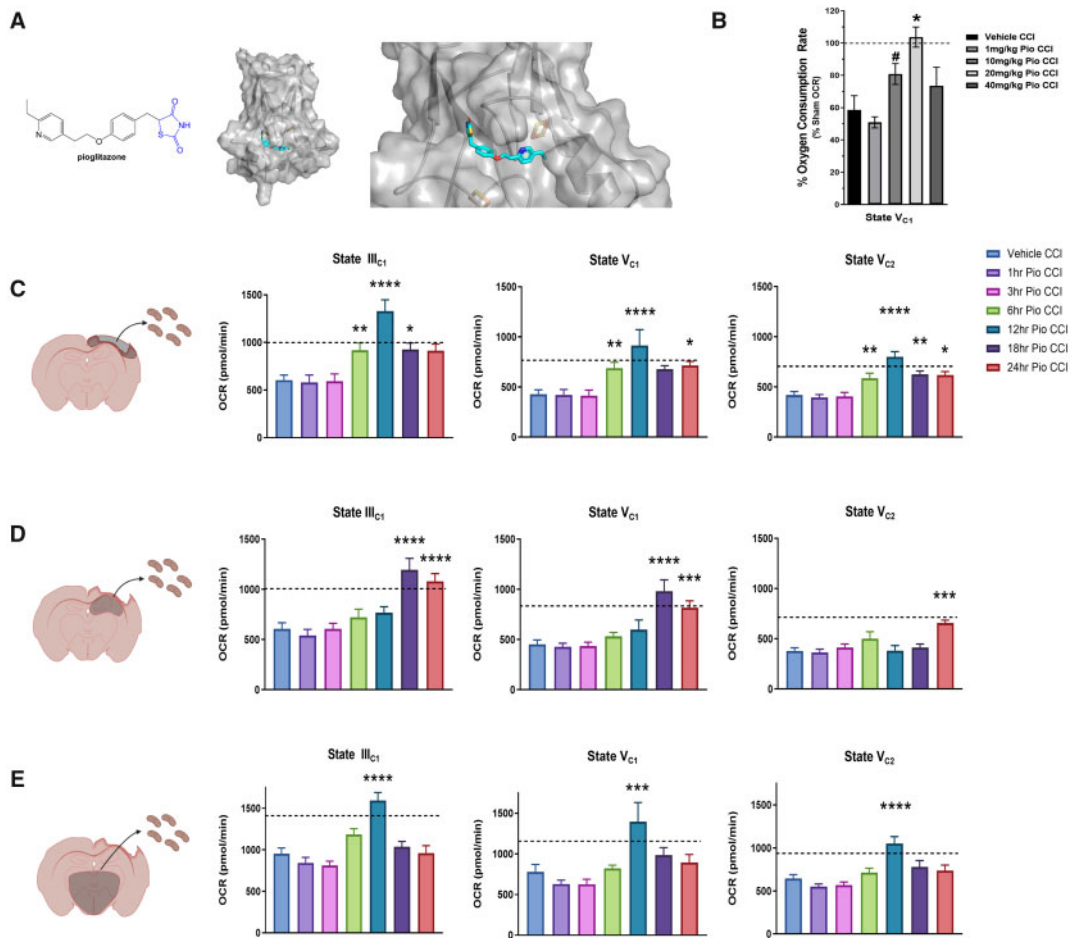


**Figure 1 Pioglitazone restores mitochondrial bioenergetics following TBI in a dose- and time-dependent manner.** (A) Chemical structure of pioglitazone and a molecular model of pioglitazone binding to the mitoNEET protein in both low and high magnification. (B) Mice received either sham surgery or severe CCI followed by pioglitazone (Pio) dosing at 15 min post-injury at either 1, 10, 20 or 40 mg/kg. Cortical mitochondria were isolated from mice at 24 h post-injury and bioenergetics were assayed using the Seahorse technology. State V complex I-mediated maximal mitochondrial respiration is not increased in 1, 10 or 40 mg/kg pioglitazone CCI groups compared to vehicle-treated CCI. After 20 mg/kg pioglitazone administration, State V bioenergetics were significantly increased compared to vehicle CCI and restored to sham levels. Line of 100% OCR corresponds to the normalized average respiration of cortical mitochondria isolated from sham-operated mice. One-way ANOVA, compared drug treated to vehicle CCI, Dunnett's *post hoc*,  $n = 4-5/\text{group}$ , mean SEM,  $F(4,17) = 12.36$ ,  $^{*}P = 0.0003$ ,  $^{*}P = 0.079$ . (C) Mice received either sham surgery or severe CCI followed by pioglitazone (20 mg/kg/day) initiated at either 1, 3, 6, 12, 18 or 24 h post-injury. An osmotic pump was inserted to ensure delivery of 20 mg/kg/day; mitochondria were then isolated from the ipsilateral cortex, ipsilateral hippocampus and limbic system at 48 h post-injury and bioenergetics were assayed using the Seahorse technology. Initiation of pioglitazone at 1 and 3 h post-injury did not increase State III mitochondrial bioenergetics in mitochondria extracted from ipsilateral cortex compared to vehicle CCI animals. However, there was a significant increase in OCR during State III<sub>C1</sub> respiration when treatment was initiated at 6, 12 and 18 h post-injury. One-way ANOVA, compared drug treated to vehicle CCI, Dunnett's *post hoc*.  $^{****}P < 0.0001$ ,  $^{**}P = 0.0086$ ,  $^{*}P = 0.0459$ , 24 h pioglitazone CCI  $P = 0.0628$ .  $F(6,97) = 9.955$ . State V complex I-mediated maximal mitochondrial OCR. Similarly, initiation of pioglitazone at 1 and 3 h post-injury did not increase State V<sub>C1</sub> mitochondrial bioenergetics while there was a significant increase in OCR when treatment was initiated at 6, 12 and 24 h post-injury. One-way ANOVA, compared drug treated to vehicle CCI, Dunnett's *post hoc*.  $^{****}P < 0.0001$ ,  $^{**}P = 0.0115$ ,  $^{*}P = 0.0372$ , 18 h pioglitazone CCI  $P = 0.0935$ .  $F(6,97) = 6.61$ . State V complex 2-mediated maximal mitochondrial OCR. Again, initiation of pioglitazone at 1 and 3 h post-injury did not increase State V<sub>C2</sub> mitochondrial bioenergetics while there was a significant increase in OCR when treatment was initiated at 6, 12, 18 and 24 h post-injury. One-way ANOVA, compared drug treated to vehicle CCI, Dunnett's *post hoc*.  $^{****}P < 0.0001$ ,  $^{**}P = 0.0097$ ,  $^{*}P = 0.0147$ .  $F(6,97) = 10.71$ . Mean SEM,  $n = 10-24/\text{group}$ . Dotted line corresponds to average sham OCR levels. (D) Initiation of pioglitazone at either 1, 3, 6 or 12 h post-injury did not increase State III mitochondrial bioenergetics in mitochondria extracted from ipsilateral hippocampus compared to vehicle CCI animals. However, there was a significant increase in OCR during State III<sub>C1</sub> respiration when treatment was initiated at 18 and 24 h post-injury. One-way ANOVA, compared drug treated to vehicle CCI, Dunnett's *post hoc*.  $^{****}P < 0.0001$ ,  $F(6,95) = 10.69$ . State V complex I-mediated maximal mitochondrial OCR. Similarly, initiation of pioglitazone at 1, 3, 6 or 12 h post-injury did not increase State V<sub>C1</sub> mitochondrial bioenergetics while there was a significant increase in OCR when treatment was initiated at 18 and 24 h post-injury. One-way ANOVA, compared drug treated to vehicle CCI, Dunnett's *post hoc*.  $^{****}P < 0.0001$ ,  $^{***}P = 0.0002$ .  $F(6,96) = 11.48$ . State V complex 2-mediated maximal mitochondrial OCR. Pioglitazone treatment starting at 1, 3, 6, 12 and 18 h post-injury did not increase State V<sub>C2</sub> mitochondrial bioenergetics while there was a significant increase in OCR when treatment was initiated at 24 h post-injury. One-way ANOVA, compared drug treated to vehicle CCI, Dunnett's *post hoc*.  $^{***}P = 0.0002$ .  $F(6,104) = 4.46$ . Mean SEM,  $n = 10-24/\text{group}$ . Dotted line corresponds to average sham OCR levels. (E) Initiation of pioglitazone at either 1, 3, 6, 18 or 24 h post-injury did not increase State III mitochondrial bioenergetics in mitochondria extracted from limbic region compared to vehicle CCI animals. However, there was a significant increase in OCR during State III<sub>C1</sub> respiration when treatment was initiated at 12 h post-injury. One-way ANOVA, compared drug treated to vehicle CCI, Dunnett's *post hoc*.  $^{****}P < 0.0001$ ,  $F(6,102) = 12.02$ . State V complex I-mediated maximal mitochondrial OCR. Similarly, initiation of pioglitazone at 1, 3, 6, 18 or 24 h post-injury did not increase State V<sub>C1</sub> mitochondrial bioenergetics while there was a significant increase in OCR when treatment was initiated at 12 h post-injury. One-way ANOVA, compared drug treated to vehicle CCI, Dunnett's *post hoc*.  $^{***}P = 0.0001$ ,  $F(6,101) = 6.13$ . State V complex 2-mediated maximal mitochondrial OCR. Pioglitazone treatment starting at 1, 3, 6, 18 and 24 h post-injury did not increase State V<sub>C2</sub> mitochondrial bioenergetics while there was a significant increase in OCR when treatment was initiated at 12 h post-injury. One-way ANOVA, compared drug treated to vehicle CCI, Dunnett's *post hoc*.  $^{****}P < 0.0001$ ,  $F(6, 102) = 8.86$ . Mean SEM,  $n = 10-24/\text{group}$ . Dotted line corresponds to average sham OCR levels.



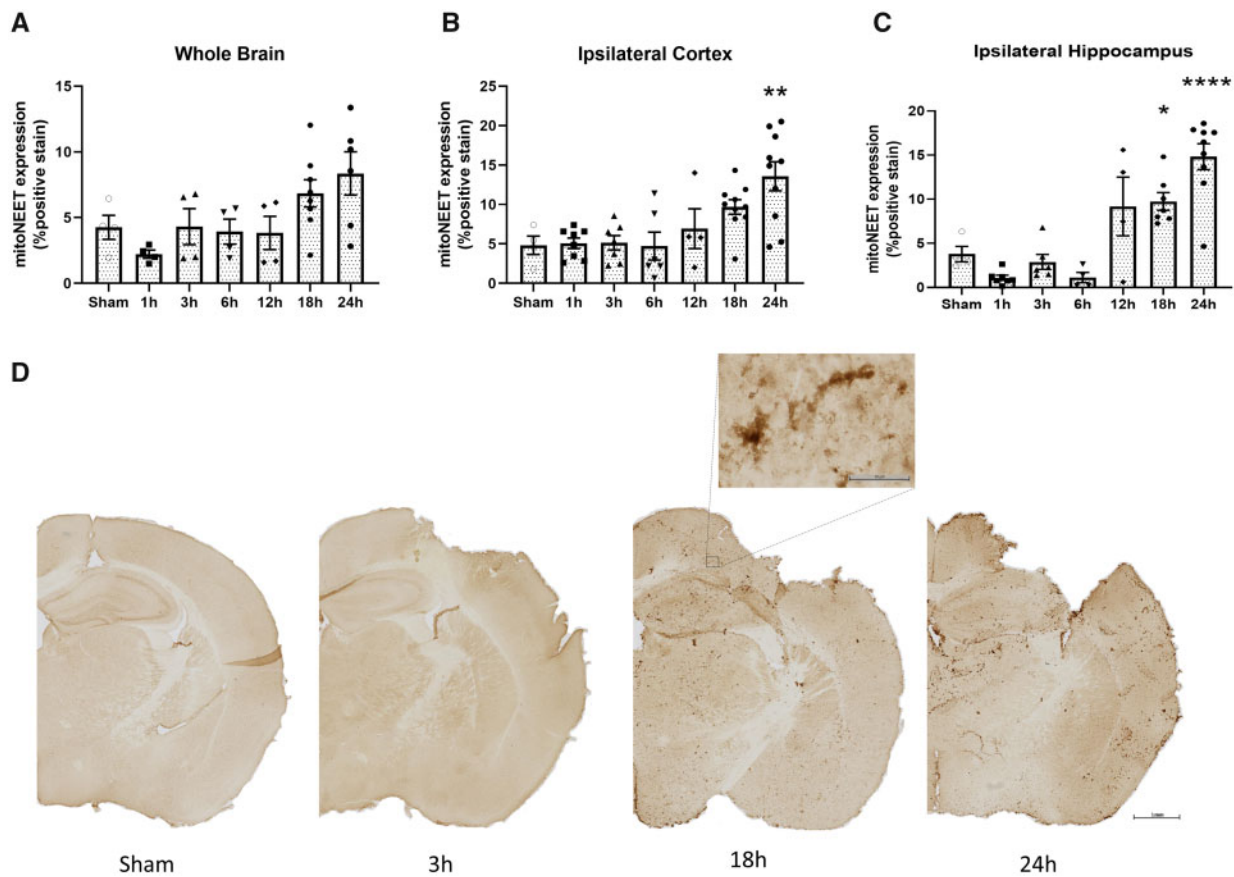


**Figure 2** Increases in mitoNEET expression are early but delayed after experimental TBI. Mice received either sham surgery or severe CCI and were euthanized at either 1, 3, 6, 12, 18 or 24 h post-injury. Brains were extracted and coronal sections underwent immunohistochemistry to measure mitoNEET expression. (A) Percentage positive mitoNEET expression in the whole brain. No significant differences were observed among groups. One-way ANOVA, compared all groups to sham, Dunnett's *post hoc*.  $F(6,27) = 3.02$ . (B) Percentage mitoNEET expression in the ipsilateral cortex. Cortical mitoNEET expression is significantly higher at 24 h post-injury compared to sham. One-way ANOVA, compared all groups to sham, Dunnett's *post hoc*.  $^{**}P = 0.002$   $F(6,42) = 6.42$ . (C) Percentage mitoNEET expression in the ipsilateral hippocampus. Hippocampal mitoNEET expression is significantly higher at 24 h post-injury compared to sham. One-way ANOVA, compared all groups to sham, Dunnett's *post hoc*.  $^{*}P = 0.03$   $^{****}P < 0.0001$ ;  $F(6,34) = 17.63$ . (D) Representative images of mitoNEET expression in sham and CCI groups (images at 1, 18 and 24 h post-injury). Scale bars = 1 mm (low magnification); 50  $\mu$ m (high magnification). Mean and individual data-points SEM,  $n = 4$ –8/group.

mitochondrial respiration when pioglitazone treatment was initiated at either 6, 12, 18 or 24 h. The greatest increase in bioenergetics for cortical mitochondria was observed when treatment was started at 12 h post-injury. Although, State IV (LEAK respiration) bioenergetics were measured, there were no differences among experimental groups, as observed in previous reports. Similar trends were observed in mitochondrial respiration profiles in both ipsilateral hippocampus and limbic regions. For hippocampal mitochondria, in general there was no significant increase in OCR with either 1, 3, 6 or 12 h initiation of pioglitazone following CCI, although there was a non-significant trend towards an increase in State  $V_{C2}$  respiration with 6 h treatment initiation (Fig. 1D). However, delayed pioglitazone treatment at either 18 or 24 h post-injury significantly increased mitochondrial bioenergetics compared to vehicle treatment. Finally, in mitochondria from the limbic region, significant increases in mitochondrial respiration were only observed when pioglitazone treatment was initiated at 12 h post-injury, although State III $_{C1}$  respiration was also significantly increased with 6 h pioglitazone initiation (Fig. 1E). With this first ever in-depth examination of the therapeutic window of pioglitazone, we find that, interestingly, early and slightly delayed treatment was not effective at restoring mitochondrial bioenergetics. Rather, delayed treatment at 12 h up to 24 h post-injury was most effective overall in restoring regional bioenergetic profiles. In fact, an independent replication confirmed this finding; pioglitazone was not effective at restoring cortical

bioenergetics with treatment delays of 1 and 3 h but was with a delay of 12 h (Supplementary Fig. 2). Given the major cognitive effects of clinical brain trauma and the central role of the hippocampus in cognition, our driving determination of optimal dosing was based on hippocampal State III $_{C1}$ -driven mitochondrial respiration. Thus, we elected to proceed with an 18 h delayed pioglitazone treatment as the optimal dosing window to use for our studies on preclinical efficacy and cognitive restoration.

### Delayed pioglitazone administration does not modulate oxidative damage after controlled cortical impact

Oxidative damage is an important pathological process following TBI and is closely related to mitochondrial function in dysfunctional cells.<sup>2,38</sup> This experiment used mitochondrial aliquots from the samples that were used for bioenergetic measurements. Blotting was performed to measure both protein carbonyls and 4-hydroxy-2-nonenal (HNE) in isolated mitochondria from ipsilateral cortex and ipsilateral hippocampus. For protein carbonyls in the ipsilateral cortex, there was a robust injury effect compared to sham (Supplementary Fig. 3). Further, a reduction in protein carbonyls measurements compared to vehicle CCI were seen regardless of when pioglitazone treatment was initiated. Conversely, pioglitazone treatment increased expression of



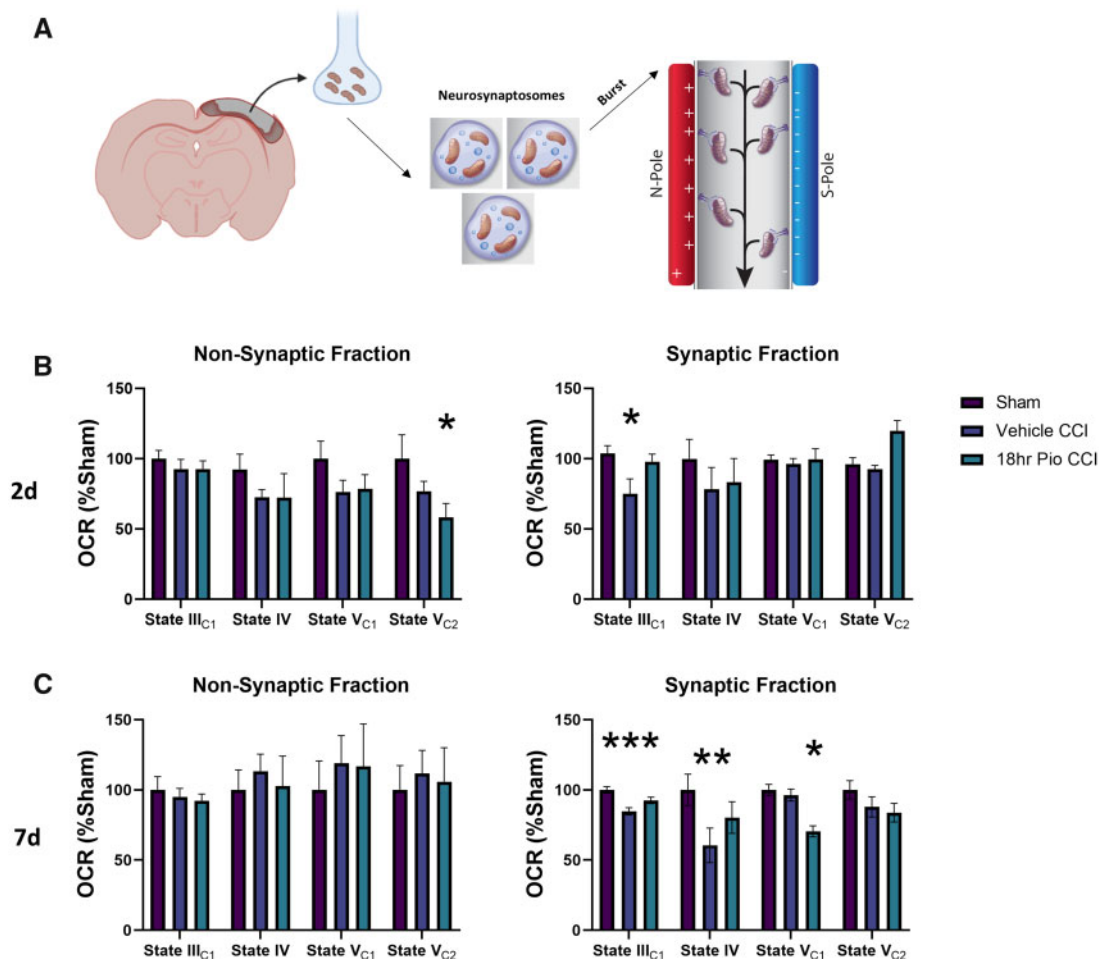


**Figure 3** Synaptic mitochondrial health in the injured cortex is restored following pioglitazone treatment initiated at 18 h following TBI. Mice received either sham surgery or severe CCI followed by vehicle or pioglitazone (20 mg/kg/day) initiated at 18 h post-injury. An osmotic pump was inserted to ensure delivery of 20 mg/kg/day. (A) Synaptic mitochondria were then isolated from the ipsilateral cortex at 2 and 7 days post-injury and mitochondrial bioenergetics were assessed. (B) Assessment of non-synaptic mitochondrial fraction at 48 h post-injury. No significant changes were observed in State III<sub>C1</sub> mitochondrial respiration. There was a significant decrease in non-synaptic State V<sub>C2</sub> respiration following 18 h pioglitazone (Pio) treatment compared to sham group. One-way ANOVA, Tukey's *post hoc*. \* $P = 0.0151$ .  $F(2,23) = 5.492$ . Assessment of synaptic mitochondrial fraction at 2 days post-injury. State III<sub>C1</sub> synaptic mitochondrial respiration was significantly lower in vehicle CCI group compared to sham while no differences were observed with the 18 h Pio group. One-way ANOVA, Tukey's *post hoc*. \* $P = 0.0309$ .  $F(2,15) = 4.225$ . (C) Assessment of non-synaptic mitochondrial fraction at 7 days post-injury. No significant changes were observed in any mitochondrial respiration state. One-way ANOVA,  $F(2,23) = 0.29$ . Assessment of synaptic mitochondrial fraction at 7 days post-injury. Synaptic State III<sub>C1</sub> and State IV mitochondrial respiration were significantly lower in vehicle CCI group compared to sham while no differences were observed with the 18 h Pio group. State V<sub>C1</sub> was significantly different in synaptic mitochondria isolated from 18 h pioglitazone-treated mice compared to sham. One-way ANOVA, Tukey's *post hoc*. \*\*\* $P = 0.0029$ , \*\* $P = 0.0011$ , \* $P = 0.0409$ .  $F(2,15) = 8.86$ . Mean SEM,  $n = 4$ –7/group. Data normalized to vehicle sham average OCR.

HNE in cortical mitochondria compared to vehicle CCI group, perhaps suggesting that increasing mitochondrial bioenergetics with pioglitazone may generate higher levels of lipid peroxidation based on higher mitochondrial activity. There were significantly lower levels of protein carbonyls and HNE in hippocampal mitochondria from 3 h pioglitazone initiation group compared to vehicle CCI, while no reduction was observed with treatment delayed until 12 or 18 h. We also determined that continuous production of free radicals is not a major mechanism at 100 days after experimental TBI, therefore pioglitazone is not influencing long-term oxidative stress (Supplementary Fig. 4). Although 3 h administration was not effective at increasing mitochondrial bioenergetics at 48 h post-injury, there may be off-target effects, such as transcriptional alterations of redox mechanisms, which result in decreased oxidative damage after 3 h pioglitazone treatment. This is plausible given the longer amount of time for these changes to influence oxidative stress. Regardless, it appears that pioglitazone treatment in general is effective at reducing oxidative

damage, especially protein carbonyls within cortical mitochondria. Levels of oxidative damage did not appear to directly influence mitochondrial bioenergetics as determined in Fig. 1.

### mitoNEET expression increases over time following controlled cortical impact in mice

To explore the availability of the mitoNEET ligand following TBI, we performed CCI surgery on wild-type mice and harvested brains at multiple time points after injury, including 1, 3, 6, 12, 18 and 24 h. Coronal sections were stained with a mitoNEET antibody and area of staining intensity was quantified. We observed higher expression surrounding the lesion site, alluding to specific targeting of injured tissue by pioglitazone (Fig. 2). Interestingly, we also observe a progressive increase in mitoNEET expression, which is significantly increased at 24 h post-injury. While there was only a trend of increased mitoNEET expression over time in the whole

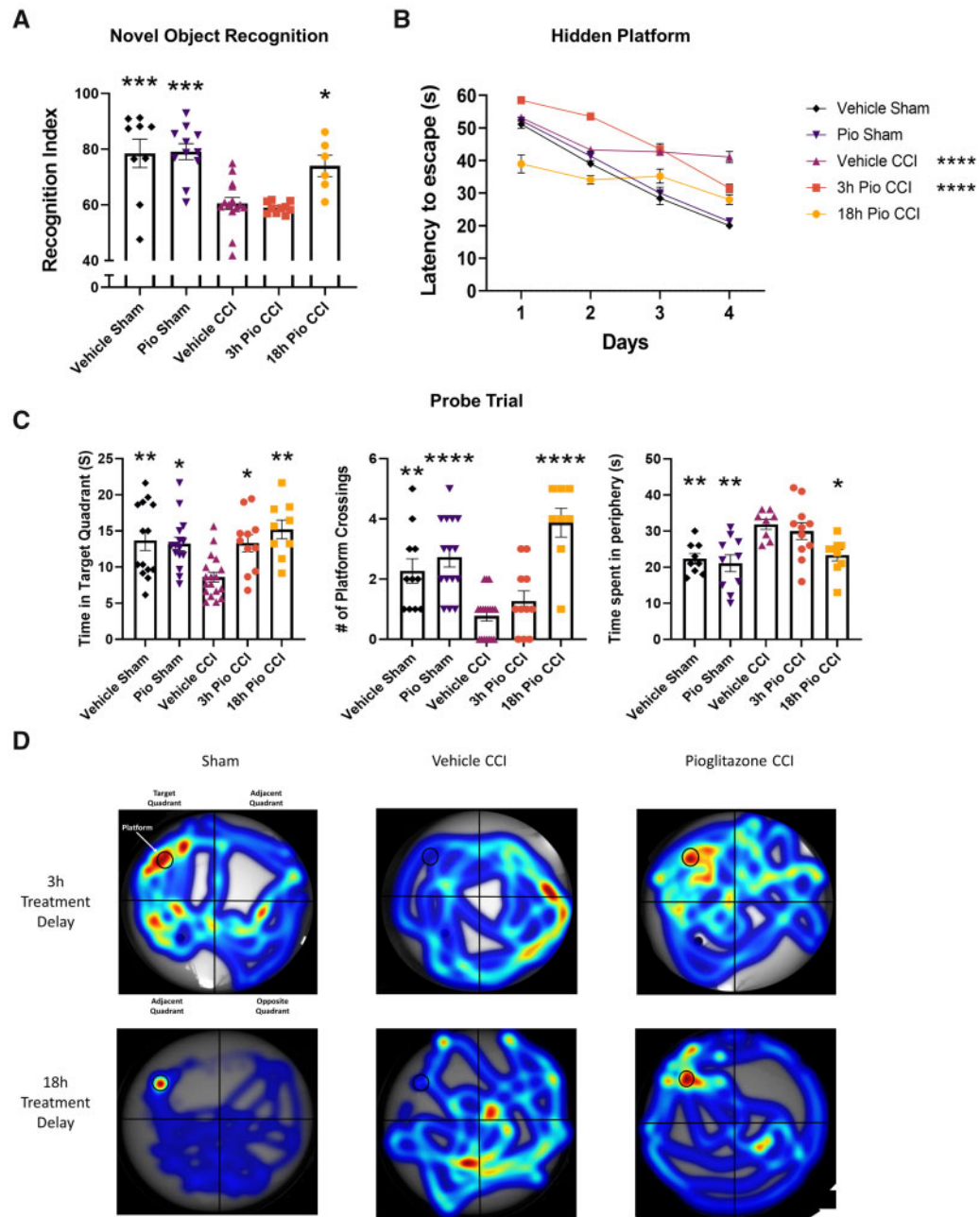


**Figure 4 Cognitive performance is improved after TBI following pioglitazone treatment initiated at 18 but not 3 h.** Mice received either sham surgery or severe CCI followed by vehicle or pioglitazone (20 mg/kg/day) initiated at either 3 or 18 h post-injury. An osmotic pump was inserted to ensure delivery of 20 mg/kg/day. Mice were given a NOR task at 8–9 days followed by MWM at 12–17 days. (A) The RI was calculated for each mouse to represent ability to remember the familiar object and explore the novel object. A score of 50 corresponds to equal object exploration. Sham groups and 18 h Pio CCI groups were significantly higher than vehicle CCI and 3 h Pio CCI groups. One-way ANOVA, Tukey’s post hoc. \*\*\* $P = 0.0001$ , \* $P = 0.0149$ ,  $F(4,42) = 15.49$ . (B) Latency to locate the hidden platform over a 4-day training period. Sham groups display progressively shorter latency time each day, demonstrating proper learning curve. Overall, vehicle CCI and 3 h Pio CCI groups displayed significantly higher latency scores compared to the vehicle sham group. Two-way ANOVA, Dunnett’s post hoc. \*\*\*\* $P < 0.0001$ ,  $F(4,243) = 68.16$ . (C) On Day 5 of MWM testing, mice explored the arena in search of the platform (probe trial). Data were calculated showing time spent in target arena compared to vehicle CCI. One-way ANOVA, Tukey’s post hoc, 18 h Pio CCI \*\* $P = 0.0010$ , vehicle sham \*\* $P = 0.0051$ , Pio sham \* $P = 0.0111$ , 3 h Pio CCI \* $P = 0.0208$ .  $F(4,62) = 6.063$ . The number of instances the platform arena was crossed was calculated, which may be a better indicator of spatial memory. Sham groups and 18 h Pio CCI had significantly higher number of crossings compared to vehicle CCI. One-way ANOVA, compared all groups to vehicle CCI, Dunnett’s post hoc. \*\*\*\* $P < 0.0001$ , \*\* $P = 0.0043$ .  $F(4,58) = 13.42$ . Peripheral tracking or scanning has been documented as a flawed search strategy for mice in finding the platform. Time circling the peripheral space was calculated to determine how mice were searching for the platform. Sham groups and 18 h Pio CCI groups has significantly lower peripheral time compared to vehicle CCI and 3 h Pio CCI groups. One-way ANOVA, Tukey’s post hoc, Pio Sham \*\* $P = 0.0019$ , vehicle sham \*\* $P = 0.0080$ , \* $P = 0.0195$ .  $F(4,42) = 5.980$ . (D) Representative heat maps of mouse activity during the probe trial showing specificity of platform tracking in the 18 h Pio CCI group. All data represent mean and individual data-points SEM,  $n = 7–10$ /group. Raw calculated data are used in all graphs.

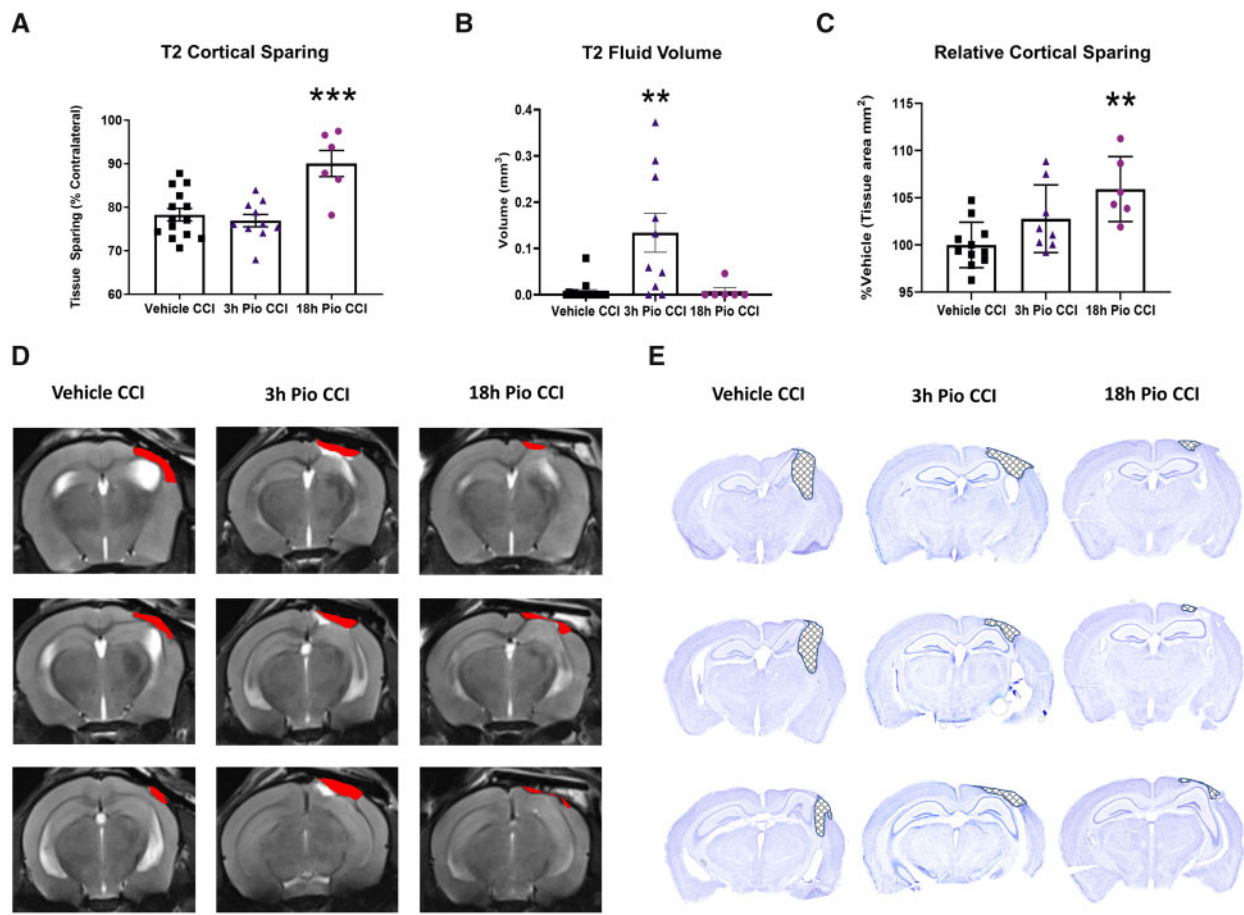


**Figure 5** Pioglitazone treatment initiated at 18 h but not 3 h, improves cortical tissue sparing. Mice received severe CCI followed by vehicle or pioglitazone (20 mg/kg/day) initiated at either 3 or 18 h post-injury. An osmotic pump was inserted to ensure delivery of 20 mg/kg/day. Mice received MRI scanning to obtain T<sub>2</sub> images at 18 days post-injury. Mice were euthanized at 21 days post-injury and tissue was analysed to assess tissue sparing on cresyl violet-stained coronal slices. (A) Initiating pioglitazone at 18 h post-injury produced significantly higher cortical tissue sparing compared to both vehicle CCI and 3 h Pio CCI groups, based on T<sub>2</sub> images. One-way ANOVA, Tukey's post hoc, \*\*\**P* = 0.0005, *F*(2,27) = 11.93. (B) Fluid volume was significantly higher for 3 h Pio CCI groups compared to vehicle CCI and 18 h Pio CCI. One-way ANOVA, Tukey's post hoc, \*\**P* < 0.008, *F*(2,30) = 10.15. (C) There was also a significant increase in tissue sparing when pioglitazone was initiated at 18 h post-injury compared to vehicle CCI, based on cresyl violet-stained tissue. Data normalized to percentage vehicle CCI group. One-way ANOVA, Tukey's post hoc, \*\**P* = 0.0027, *F*(2,22) = 7.355. (D) Representative serial coronal sections (bregma -1.6, -2.05, -2.5 mm) outlining the lesion area in red. (E) Representative serial coronal sections outlining the lesion area are highlighted with cross-hatching. Mean and individual data-points SEM. *n* = 7–10/group.

brain, this result was amplified on investigation of expression in the ipsilateral hippocampus and cortex. Indeed, mitoNEET expression steadily increases and was significantly higher by 24 h post-injury. These data confirm that delayed treatment could increase mitochondrial bioenergetics by harnessing the progressively elevated levels of mitoNEET expression after CCI.

### Synaptic mitochondrial health after pioglitazone administration

Our group has established a new technique for isolating and assessing synaptic mitochondrial profiles.<sup>27</sup> With this capability, we can isolate synaptic mitochondria from the ipsilateral cortical punch and examine bioenergetics. Past research has demonstrated that synaptic mitochondria in general are particularly susceptible to cellular stress following brain injury<sup>39,40</sup> and restoration of mitochondrial function in the synapse after an insult is critical for neurotransmission.<sup>41</sup> To examine whether initiation of pioglitazone treatment at 18 h promotes ongoing synaptic recovery in the injured cortex, we isolated mitochondria from the neuronal synapse at both 2 and 7 days following CCI (Fig. 3). At 2 days post-injury, non-synaptic mitochondria from the injured cortex had

lower State V<sub>C2</sub> respiration following 18 h pioglitazone treatment compared to the sham group. In the synaptic mitochondrial fraction, there was a decrease in State III<sub>C1</sub> bioenergetics in vehicle-treated CCI animals compared to the sham group at 2 days post-injury. Pioglitazone treatment, delayed to 18 h after injury, restored this bioenergetic deficit in synaptic mitochondria. Importantly, we again observe a State III<sub>C1</sub> synaptic mitochondrial bioenergetic drop in vehicle-treated animals compared to the sham group at 7 days post-injury. There is no significant difference in sham and 18 h pioglitazone-treated CCI cortical synaptic mitochondrial State III<sub>C1</sub> respiration at 7 days post-injury. This improvement indicates ongoing restoration of metabolism related to neurotransmission. As deficits in neurotransmission relate to neurological performance, the effects of delayed pioglitazone treatment on neurobehavioural outcomes were explored next.

### Assessing cognitive recovery following pioglitazone administration after controlled cortical impact

To link early improvement in mitochondrial function to subacute neurobehavioural outcomes, we compared cohorts of mice that had been given pioglitazone at either 3 or 18 h following



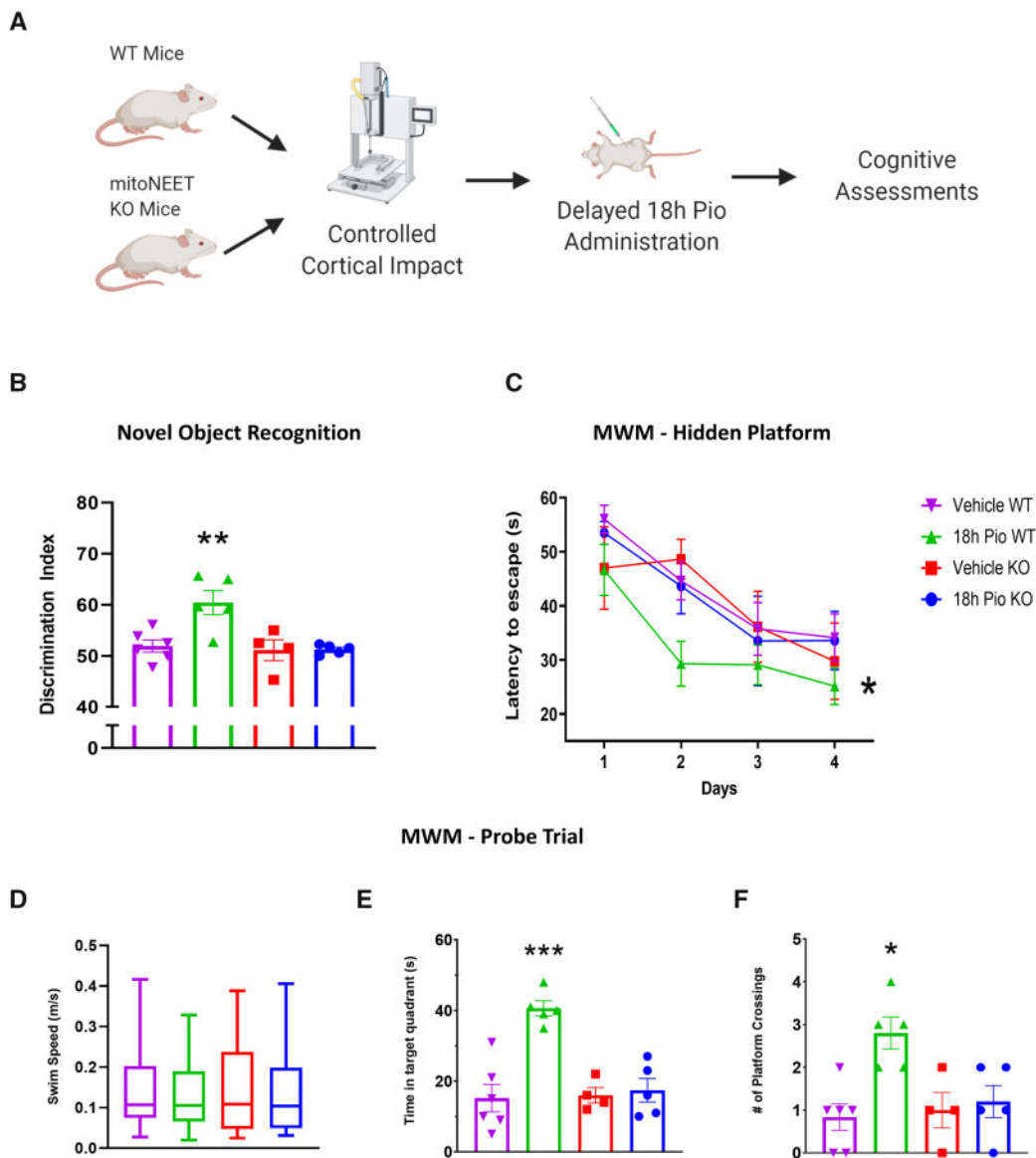


**Figure 6 Pioglitazone restores cognitive function in wild-type mice but not mitoNEET null mice.** (A) C57Bl/6 or mitoNEET null female and male mice received severe CCI followed by vehicle or pioglitazone (20 mg/kg/day) initiated at 18 h post-injury. An osmotic pump was inserted to ensure delivery of 20 mg/kg/day. Mice were given a NOR task at 3 days followed by MWM from 7 to 11 days following CCI. (B) The RI was calculated for each mouse to represent the ability to remember familiar objects and explore a novel object. A score of 50 corresponds to equal object exploration. The 18 h Pio wild-type (WT) group had significantly higher scores than 18 h vehicle WT, while there were no differences between the mitoNEET knockout groups. One-way ANOVA, Tukey's *post hoc*. \*\* $P = 0.0075$ ,  $F(3,16) = 7.528$ . (C) Latency to locate the hidden platform over the 4-days training period. The 18 h Pio WT group was significantly different compared to the 18 h vehicle WT group while no differences were seen in the mitoNEET knockout groups. Two-way ANOVA, Tukey's *post hoc*. \* $P = 0.0177$ ,  $F(3,64) = 3.490$ . (D) On Day 5 of MWM testing, mice explored the arena in search of the platform. Swim speed was unchanged between all treatment groups. One-way ANOVA,  $F(3,16) = 0.24$ . (E) Data were calculated showing time spent in target quadrant (platform arena). 18 h Pio WT had significantly higher time spent in target arena compared to 18 h vehicle WT and no differences were found between mitoNEET knockout groups. One-way ANOVA, Tukey's *post hoc*, \*\*\* $P = 0.0005$ ,  $F(3,16) = 14.70$ . (F) During the fifth day probe trial, the number of instances the platform arena was crossed was calculated. Again, 18 h Pio WT had significantly higher platform crossings compared to 18 h vehicle WT and no differences were found between mitoNEET knockout groups. One-way ANOVA, Tukey's *post hoc*. \* $P = 0.0295$ ,  $F(3,16) = 6.398$ . All data represent either mean and individual data-points SEM or box and whisker (median, interquartile interval, max, min),  $n = 5$ –6/group. Raw calculated data are used in all graphs.

experimental TBI. We used the NOR test to examine short-term memory in mice at 8–9 days following TBI. The RI is used to assess the animal's preference for the novel object, representing functional memory of the familiar object. The 18 h pioglitazone (Pio) CCI group had significantly higher RI scores compared to vehicle CCI and 3 h Pio CCI and was not significantly different from shams (Fig. 4). We found similar cognitive improvements after 18 h pioglitazone treatment in a model of mild-to-moderate TBI, although improvements were less pronounced (Supplementary Fig. 5). The

MWM test has long been used in TBI research due to robust detection of learning and memory deficits.<sup>42</sup> Overall, the 18 h Pio CCI group had significantly lower latency to locate the hidden platform over the four training days compared to vehicle CCI and 3 h Pio CCI and was not significantly different from sham groups. Two common parameters that dictate cognitive performance during the probe trial are the latency to locate and rest on hidden platform and time spent in platform quadrant during the fifth day probe trial. As such, we report both parameters. Accounting for latency

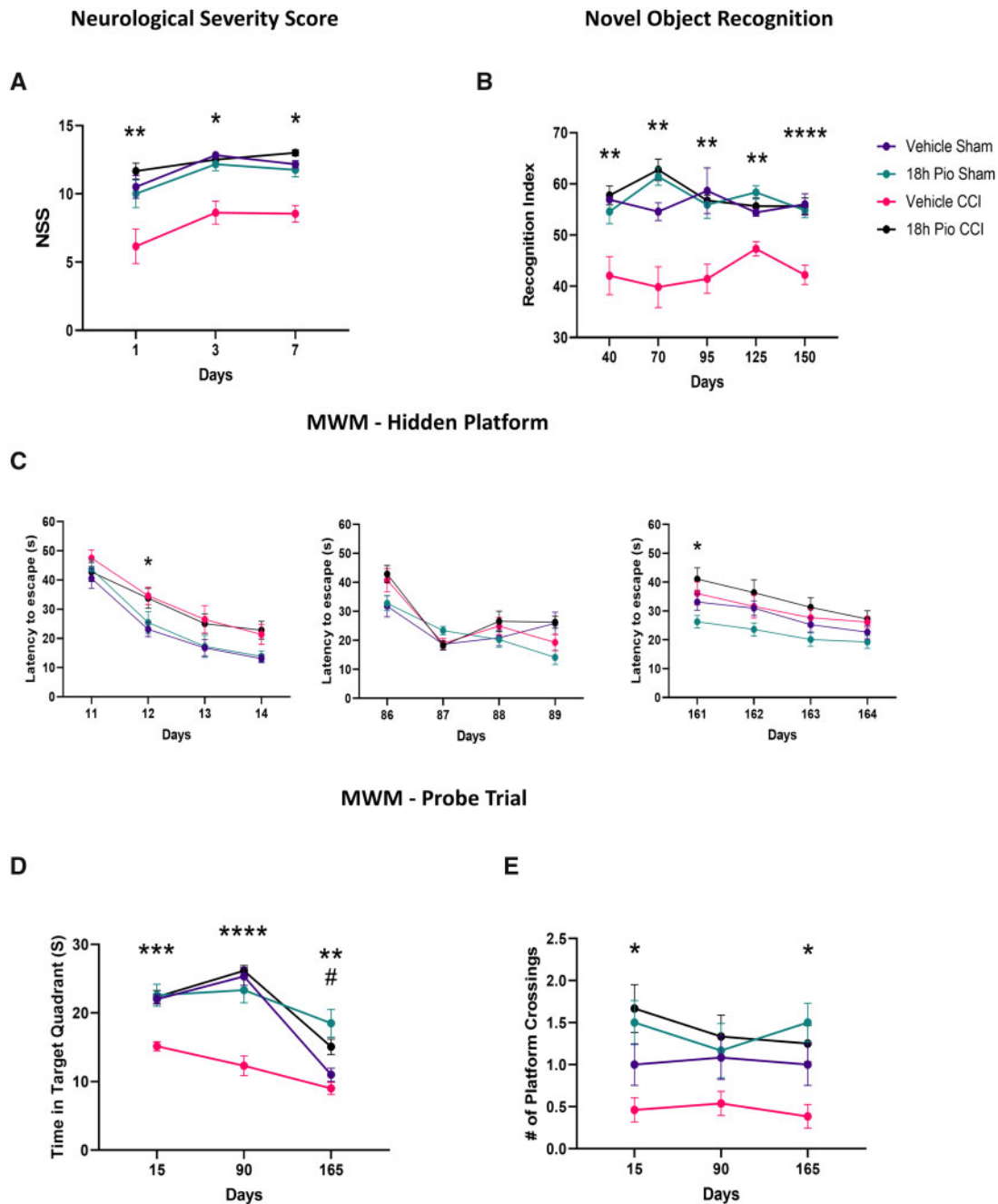


**Figure 7** Chronic improvements in cognitive recovery after delayed pioglitazone treatment following TBI. Male and female mice received either sham surgery or severe CCI followed by vehicle or pioglitazone (20 mg/kg/day) initiated at 18 h post-injury. An osmotic pump was inserted to ensure delivery of 20 mg/kg/day. Mice were tasked with acute motor function assays, NSS, assayed at 1, 3 and 7 days post-injury. Further, they underwent the NOR task at 30, 60, 90, 120 and 150 days post-injury as well as MWM at 14, 90 and 160 days post-injury. (A) NSS was calculated based on the composite score for the beam-walking task. The 18 h Pio CCI group were significantly higher than vehicle CCI at each time point, while sham groups were higher than vehicle CCI at 3 days and 7 days post-injury. Kruskal–Wallis test, Dunn’s post hoc. 1 day:  $**P = 0.01$  18 h Pio CCI versus vehicle CCI, Kruskal–Wallis = 11.10; 3 days:  $*P < 0.018$ , Kruskal–Wallis = 18.50; 7 days:  $*P < 0.026$ , Kruskal–Wallis = 21.39. (B) The RI was calculated for each mouse with a score of 50 corresponding to equal object exploration. Sham groups and the 18 h Pio CCI group were consistently significantly higher than the vehicle CCI group at all time points. One-way ANOVA, Tukey’s post hoc. 30 days:  $**P < 0.005$ ,  $F(3,45) = 8.833$ ; 60 days:  $**P < 0.002$ ,  $F(3,45) = 16.38$ ; 90 days:  $**P < 0.007$ ,  $F(3,45) = 7.205$ ; 120 days:  $**P < 0.002$ ,  $F(3,45) = 13.40$ ; 150 days:  $****P < 0.0001$ ,  $F(3,45) = 14.67$ . (C) Latency to locate the hidden platform over a 4-days training period. The 18 h sham group display a progressively shorter latency time amongst all training days demonstrating a proper learning curve. There is a significant injury effect on Days 12 and 161 in the hidden platform trial, demonstrating ongoing deficits in learning. One-way repeated measures ANOVA, Tukey’s post hoc. 14 days:  $*P = 0.036$ . Treatment main effect  $F(3,45) = 5.450$ ; 90 days: treatment main effect  $F(3,45) = 2.237$ ; 160 days:  $*P = 0.020$ . Treatment main effect  $F(3,45) = 3.264$ . (D) On Day 5 of MWM testing, mice explored the arena in search of the platform. Data were calculated showing time spent in the target quadrant (platform arena). At 14 and 90 days post-injury, all sham and treatment groups had significantly higher time spent in target arena compared to vehicle CCI. At 160 days, pioglitazone-treated groups have a higher time in target quadrant compared to vehicle CCI. One-way ANOVA, Tukey’s post hoc, 14 days:  $***P < 0.0002$ ,  $F(3,45) = 12.44$ ; 90 days:  $****P < 0.0001$ ,  $F(3,45) = 22.35$ ; 160 days: 18 h Pio groups compared to vehicle CCI  $**P < 0.01$ , 18 h Pio sham versus vehicle sham  $*P = 0.0013$   $F(3,45) = 10.55$ . (E) Additionally, the number of instances the platform arena was crossed was calculated. Sham groups and 18 h Pio CCI had significantly higher number of crossings compared to vehicle CCI. One-way ANOVA, Tukey’s post hoc, 14 days: 18 h Pio groups versus vehicle CCI  $*P < 0.016$ ,  $F(3,45) = 5.39$ ; 90 days:  $F(3,45) = 1.957$ ; 160 days: 18 h Pio groups versus vehicle CCI  $*P < 0.026$   $F(3,45) = 5.335$ . All data represent mean SEM,  $n = 12$ –13/group. Raw calculated data are used in all graphs.

scores on all days, the 18 h Pio CCI group had significantly lower latency scores compared to vehicle CCI and 3 h Pio CCI groups and was not significantly different from shams. For time spent in the platform arena, all sham and pioglitazone-treated groups had higher platform arena exploration time compared to vehicle CCI group. However, sham groups and the 18 h Pio CCI group had higher number of platform crossings during the fifth day probe trial compared to vehicle CCI, while the 3 h Pio CCI group was not different from vehicle CCI group. As described previously, repetitive looping, including thigmotaxic searching and peripheral looping, is one of the most inefficient strategies for finding the platform and is used in mice with cognitive disorders.<sup>43</sup> Further, mice use inefficient strategies and peripheral looping at a higher rate following experimental TBI. To assess where mice are scanning for the platform, we analysed mouse location among different groups. We found that both vehicle CCI and 3 h Pio CCI groups had significantly higher peripheral scanning time compared to sham and 18 h Pio CCI groups, implying flawed search strategies. Overall, 18 h initiation of pioglitazone treatment after TBI has a profound effect on the restoration of memory and learning capabilities while initiation of treatment at 3 h has little effect on cognition after TBI.

### Initiation of pioglitazone at 18 h results in neuroprotection following traumatic brain injury

Mice were scanned at 18 days post-injury using MRI to obtain T<sub>2</sub>-weighted coronal images to assess cortical sparing and oedematous tissue following TBI. The 18 h Pio CCI group had significantly higher cortical tissue sparing compared to vehicle CCI and 3 h Pio CCI groups (Fig. 5A). Representative T<sub>2</sub> images depict lesion areas for all groups. The incidence of hippocampal deformation is commonly observed in the CCI model, especially those with a flat-tip impactor.<sup>44</sup> We also examined oedema around the lesion site after CCI and pioglitazone treatment. Thiazolidinediones have long been shown to contribute to systemic oedema as a major side effect of treatment.<sup>45,46</sup> Since it is also known that vasogenic oedema results in morbidity following TBI,<sup>47</sup> oedema was measured at the lesion site following pioglitazone treatment. We found that 18 h initiation of pioglitazone was consistent with statistically lower levels of oedema compared to 3 h initiation of pioglitazone (Fig. 5B). This may be a clinically relevant side effect of early pioglitazone administration, which highlights another important reason for delayed treatment. Further, we assessed cortical sparing on post-mortem coronal sections as an independent replication of MRI data; staining with cresyl violet can also define the neuronal border with greater detail (Fig. 5D). Using a subset of mice from the MRI scans, we observe that 18 h Pio CCI groups had significantly higher tissue sparing compared to vehicle CCI group, while there are no differences in the 3 h Pio CCI group. Representative cresyl violet-stained sections demonstrate increased cortical sparing in the 18 h Pio CCI group. Here, we demonstrate that delaying pioglitazone treatment results in greater neuroprotection following TBI.

### Determine whether mitoNEET is the primary therapeutic target with delayed pioglitazone treatment

Our group has previously shown that mitoNEET is the main therapeutic target for pioglitazone following experimental TBI when treatment is initiated immediately following injury.<sup>11</sup> We performed an independent confirmation of these results in the current study (Supplementary Fig. 6). To show that mitoNEET is the primary target after delayed pioglitazone treatment, we performed a study to examine the effects of delayed pioglitazone treatment

at 18 h post-injury on both wild-type and mitoNEET null mice. We demonstrate that 18 h delayed administration of pioglitazone produces cognitive recovery following CCI in wild-type mice, as observed in both NOR and MWM paradigms (Fig. 6). Further, we observe that this treatment does not benefit cognition in mitoNEET null mice. This holds true for RI scores during the NOR test as well as latency to find the platform during the MWM probe trial. These results provide strong rationale that mitoNEET binding is driving therapeutic benefit following pioglitazone administration.

### Lasting cognitive restoration with delayed pioglitazone treatment after traumatic brain injury

On our determination that 18 h initiation of pioglitazone functions via mitoNEET and is effective at early and subacute time points, we then wanted to examine the ongoing and chronic cognitive and neuroprotective therapeutic benefits. Using the NSS beam-walking assay, we saw that delayed pioglitazone treatment improves early recovery of motor function (Fig. 7). Further, we then examined longitudinal effects on cognition using both NOR and MWM. Remarkably, we observed lasting therapeutic benefit of pioglitazone after TBI on RI during the NOR task. Sham groups and 18 h Pio CCI consistently displayed higher RI scores compared to vehicle-treated CCI mice. Although RI scores were lower than in the subacute study, one-sample t-tests at each time point revealed that sham groups and 18 h Pio CCI group were significantly higher than chance performance (50%), indicating memory of the familiar object.<sup>48</sup> Finally, the probe trial of the MWM paradigm revealed that again delayed pioglitazone treatment improves memory retention following TBI, measured by time in target quadrant. This is also exemplified by higher number of platform crossings in sham groups and 18 h Pio CCI compared to vehicle-treated CCI group. There were only minor injury deficits in hidden platform learning compared to sham groups.

### Delayed pioglitazone treatment reduces brain atrophy

Using MRI T<sub>2</sub>-weighted imaging, we examined the effect of delayed pioglitazone treatment using tensor-based analysis of whole brain, an unbiased technique with which to determine changes in ongoing neuroprotection and brain atrophy. Data were spatially coregistered to an age-matched, study-specific mean template brain and the resulting deformation field was used to calculate local increases and decreases in tissue deformation, referred to as tissue swelling/expansion and atrophy/compression, respectively (Fig. 8). Both brain local tissue swelling/expansion and atrophy/compression were predominantly confined to ipsilateral cortex, hippocampal and thalamic regions in all injured mice. As the injury progressed, the degree of brain atrophy/compression reduced over time (from 30 to 100 days) for both CCI groups, at 166 days it was confined to the ipsilateral cortex and hippocampus. Brain swelling/expansion showed a similar trajectory, albeit over a more delayed time course. We found that sham and TBI groups were significantly different at all post-injury time points, as expected. Furthermore, at 100 days post-injury, pioglitazone treatment resulted in significantly decreased brain atrophy as compared to vehicle-treated CCI group, but brain swelling/tissue expansion was similar among both CCI groups.

## Discussion

As stated previously, we have shown that pioglitazone demonstrates therapeutic efficacy in multiple models of TBI and further, has been shown to be dependent on the presence of mitoNEET in



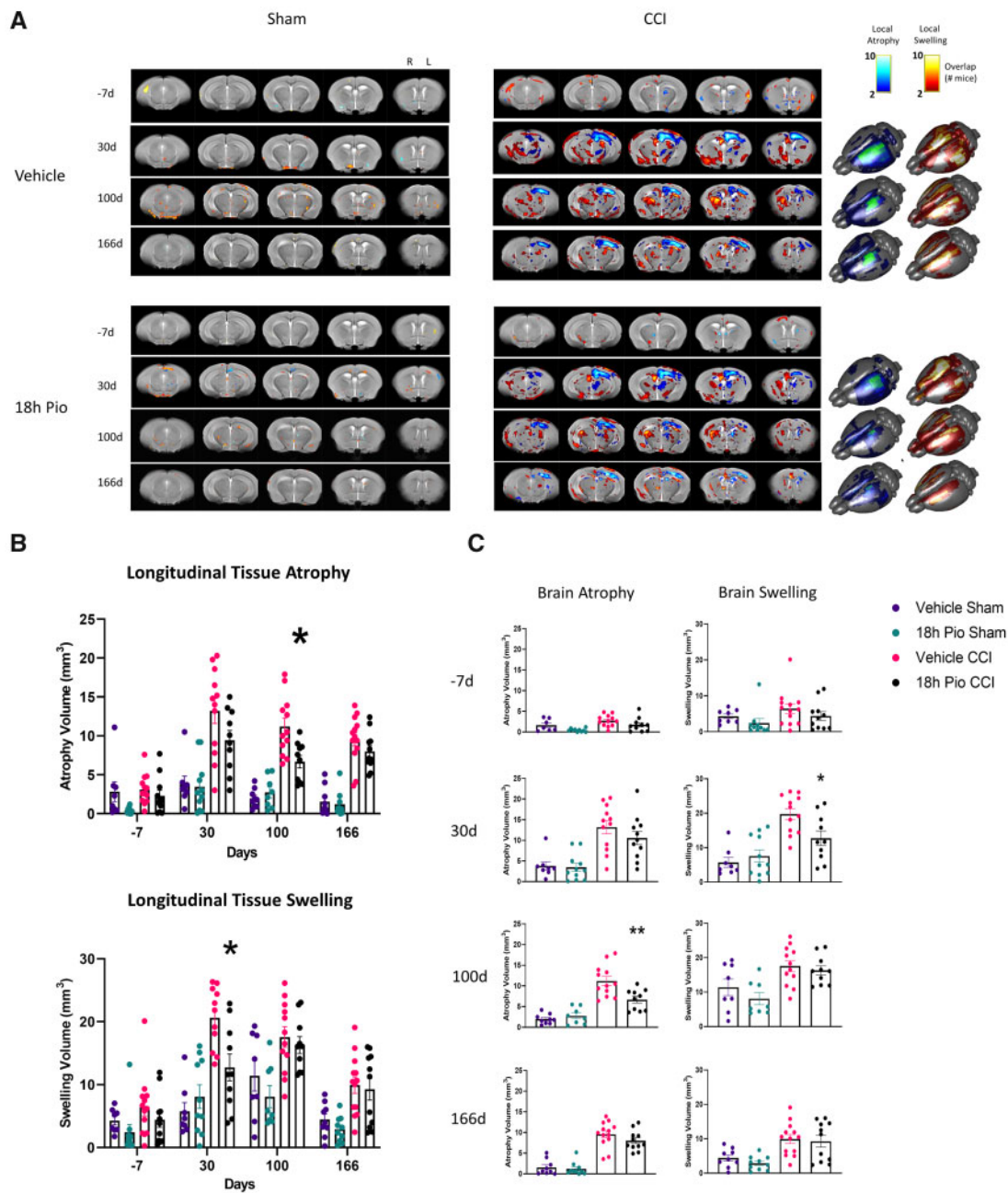


**Figure 8** Longitudinal tracking of brain atrophy reveals therapeutic benefit of 18 h delayed pioglitazone treatment after TBI. Male and female mice received either sham surgery or severe CCI followed by vehicle or pioglitazone (20 mg/kg/day) initiated at 18 h post-injury. An osmotic pump was inserted to ensure delivery of 20 mg/kg/day. MRI scanning was performed at -7, 30, 100 and 166 days post-injury. (A) Overlap maps of local tissue deformation (atrophy, swelling) from all mice at all time points after injury projected on to the mean deformation image. Brighter red and blue colours on coronal slices (approximately -4 to 0 mm bregma; spaced 1 mm apart) correspond to higher number of mice that display swelling and atrophy, respectively. (B) There were significant differences in brain atrophy between sham and CCI groups at all time points except for -7 days [ $P < 0.02$ ;  $F(3,40) = 40.74$ ]. In addition, pioglitazone-treated CCI mice had significantly less brain atrophy compared to vehicle-treated CCI mice at 100 days post-injury [ $*P = 0.0172$ ;  $F(3,40) = 40.74$ ]. There were significant differences in brain swelling between 18 h Pio sham and CCI groups [ $P < 0.02$ ;  $F(3,40) = 20.88$ ] at 100 and 166 days post-injury, although there was only a significant difference between 18 h Pio sham and vehicle CCI at 30 days post-injury. In addition, there was a significant difference between CCI groups at 30 days post-injury [ $P = 0.035$ ;  $F(3,40) = 20.88$ ]. (C) Atrophy and swelling data displayed according to time point. Again, the only difference between CCI groups was for brain atrophy and brain swelling at 30 days post-injury. All data represent mean and individual data-points SEM,  $n = 8$ –12/group. Raw calculated data are used in all graphs.

both TBI<sup>11</sup> and spinal cord injury.<sup>21</sup> In this article, we build on these findings to show that the optimal dose of pioglitazone for restoring mitochondrial function has a delayed therapeutic window that could be translationally very significant for brain trauma victims. In fact, we show that long-term neuroprotection and

cognition recovery are improved when pioglitazone treatment is delayed to 18h, when compared to a 3h therapeutic delay. This again shows that mitochondrial dysfunction after TBI is an important pathological target and has an extended therapeutic window after brain injury. Finally, we causatively show that behavioural

improvement is a product of mitoNEET targeting, utilizing mitoNEET null transgenic model.

Pioglitazone is a well-known ligand for PPAR and likely exerts some pharmacological manipulation through this pathway. In pre-clinical TBI studies, early reports on pioglitazone and other 'glitazones' as a therapeutic agent for TBI focused on potential anti-inflammatory effects mediated through PPAR that could quell secondary injury cascades. It has been shown that rosiglitazone and other PPAR agonists, such as fenofibrate, mitigate inflammation and oxidative damage after experimental TBI to afford neuroprotection.<sup>49–53</sup> Further, PPAR- $\gamma$  has been a therapeutic target for restoring mitochondrial function in the context of neurological disease, based on molecular changes related to bioenergetics, metabolism, mitochondrial biogenesis and redox balance.<sup>54</sup> We have shown that targeting PPAR- $\gamma$  coactivator-1 $\alpha$  (PGC-1 $\alpha$ ) increases mitochondrial content and exerts neurobehavioural benefits following TBI.<sup>10</sup> However, our group has previously shown that pioglitazone can generate improvement in mitochondrial bioenergetics 1 h after administration showing that pioglitazone produces fast-acting effects, not mediated through PPARs activation and subsequent transcription modifications.<sup>11</sup> Further, we have previously shown,<sup>11</sup> and confirm in the current studies, that significant improvement in neuroprotection and cognitive function is dependent on the presence of mitoNEET, revealing that mitoNEET is a critical target of pioglitazone after TBI. We also confirm that mitoNEET-dependent pioglitazone therapy is not due to phenotypic changes in the mitoNEET null model as there are no significant differences in body weight, brain mitochondrial bioenergetics (data not shown), or swim speed (Fig. 6D) between mitoNEET null mice and wild-type mice at 3 months of age.

mitoNEET is important in redox- and pH-sensing and regulates mitochondrial function.<sup>23</sup> mitoNEET overexpression in white adipose tissue also results in significantly increased PGC-1 $\alpha$  expression, which promotes mitochondrial biogenesis.<sup>22</sup> A recent study by Zuris *et al.*<sup>55</sup> demonstrated pioglitazone-mitoNEET binding was able to inhibit iron-sulphur cluster transfer; however, this role in the context of CNS injury has been unexplored. It is known that when pioglitazone is pharmacologically active, it binds mitoNEET, which can be described as a switch phenomenon, whereas oxidative phosphorylation is stimulated and mitochondrial bioenergetics are increased. After insult and cellular stress, mitochondria, which are overloaded with calcium and produce high levels of reactive oxygen species, appear to switch themselves off via mitoNEET, turning to a glycolytic state. In fact, hyperglycolysis is a well-defined pathophysiology following clinical and preclinical TBI.<sup>56,57</sup> Pioglitazone-mitoNEET binding may shift cellular metabolism in the brain early after TBI, leading to improved and more balanced energy production and enhanced cell survival. It is possible this shift could also attenuate the extent of lactate build up in neurons, which is associated with poor outcome after TBI.<sup>58</sup> In corroboration with this, we observed lasting restoration of State III bioenergetics in synaptic mitochondria isolated from the ipsilateral cortex, showing that targeted pioglitazone treatment specifically acts on synaptic metabolism.

Remarkably, mitochondrial bioenergetics are significantly improved when initial administration begins at 12 h but not at 1, 3 or 6 h. This suggests that there is a post-injury temporal window within which mitochondria cannot be optimally stimulated after injury. From our previous work<sup>12</sup> and [Supplementary Fig. 6](#), we know that immediate (15 min) administration of pioglitazone rescues mitochondrial function, imparts neuroprotection and improves cognition after TBI. These results in conjunction with the current study indicate that there is a biphasic, extended treatment window in which pioglitazone could be administered to maintain mitochondrial homeostasis after TBI. Indeed, our research group previously demonstrated that cyclosporin A has a

similar temporal therapeutic window, showing neuroprotective ability in the first hours after injury and again at 24 h following TBI.<sup>6,59</sup> Understanding the temporal therapeutic potential for a druggable target is critical for adequate preclinical drug development.<sup>36</sup> Indeed, promising therapeutics may be inadequately tested based on underdeveloped pharmacodynamic and biological profiles. Therapeutic crossing of the blood-brain barrier is a challenge made easier by pathological blood-brain barrier opening after TBI but again this time course is important for treatment paradigms. Here, we show unprecedented bioenergetic recovery and neuroprotection following delayed therapeutic treatment of pioglitazone, even up to 18 and 24 h following experimental TBI. Further, pioglitazone may be effective even later than 24 h after injury, which was the longest delay examined in the current study. While unexpected, these data could have major implications on important early intrinsic changes in mitochondrial dynamics.

We hypothesize that changes in mitoNEET expression could drive this biphasic treatment window and we are currently working to elucidate this mechanism. Iron deposition occurs following brain injury, especially in areas of microhemorrhage and blood-brain barrier breakdown, and dysregulation can induce ferroptosis leading to worsened outcome after TBI.<sup>60,61</sup> As mitochondria use iron and, in fact mitoNEET contains iron, it is possible that iron deposition around the cortical lesion steadily promotes higher expression of mitoNEET. In turn, pioglitazone can hijack this pathological occurrence to generate enhanced bioenergetics around the injury. While the delayed therapeutic effects could be a product of mitoNEET availability after injury, this would not be a major cause as we employ continuous treatment once pioglitazone is initiated. Although it is possible that mitoNEET binding by pioglitazone early after injury could affect ongoing changes in mitoNEET expression.

Based on recent findings, it is likely that mitochondrial dynamics contribute to the understanding of the therapeutic window of mitochondrial-directed drugs. In response to mitochondrial damage, several dynamic processes and modifications, including mitochondrial biogenesis, fusion, fission and mitophagy, are used by the cell to control mitochondrial quality and to promote cell survival.<sup>62,63</sup> Overexpression of mitoNEET in adipose tissue has been shown to increase the expression of PGC-1 $\alpha$ , which can increase mitochondrial number and biogenesis.<sup>64</sup> mitoNEET is crucial to the mitochondrial network and inactivation of mitoNEET has been shown to reduce inter-mitochondrial junctions, leading to impaired mitochondrial respiration.<sup>65</sup> Therefore, it is possible that mitoNEET stabilization by pioglitazone could promote mitochondrial function, in part, by integration of the mitochondrial network. Another crucial intracellular mechanism, mitophagy, is a way to identify and systematically remove damaged mitochondria to ensure adequate energy supply and function of the cell. Recent report by Chao *et al.*<sup>66</sup> demonstrates that early mitophagic events are crucial for ongoing neuroprotection after TBI.<sup>67</sup> In this study, inhibiting mitophagy results in worsened outcomes, supporting the early reparative role of mitophagy in clearing of damaged mitochondria before initiation of apoptotic pathways. We hypothesize that pioglitazone, when administered early after CCI, could preserve dysfunctional mitochondria that are destined for early mitophagy, thereby creating ongoing metabolic deficiency. Indeed, it is known that mitoNEET plays a direct role in Parkin-mediated mitophagy.<sup>68</sup> It is possible, therefore, that pioglitazone, targeting mitoNEET, can be administered at an inopportune time pathologically when intrinsic mitochondrial regulation pathways, such as mitophagy, are in effect. Delaying treatment until 18 h post-injury allows necessary mitochondrial dynamics acutely after TBI while promoting mitochondrial function in critical phases of secondary injury.

Importantly, these data indicate that mitochondrial dysfunction following TBI may not be a result of mitochondrial failure due to oxidative damage as previously hypothesized. Oxidative damage in mitochondria appears to increase acutely following TBI with a peak at 3 days post-injury.<sup>38</sup> Here, we show that mitochondrial dysfunction precedes this peak and bioenergetic improvements by pioglitazone occur by 2 days post-injury. According to Supplementary Fig. 3, mitigation of oxidative stress does not seem to be a determinant of long-term cognitive outcome, as levels of oxidative damage are lower after 3 h initiation of pioglitazone. Free radical accumulation in mitochondria can react with polyunsaturated fatty acids to form lipid peroxidation, creating aldehyde by-products such as HNE.<sup>69</sup> When free radicals interact with vulnerable amino acids protein carbonylation can also occur after TBI.<sup>70</sup> Pioglitazone is fast acting and in fact, could prevent some of the redox-sensing capabilities of mitoNEET, thereby potentially producing more oxidative stress over time. Further, greater mitochondrial activity in damaged mitochondria can naturally drive increased free radical production, potentially explaining the increases in HNE in the cortex following delayed pioglitazone administration after experimental TBI. Probably, 3 h initiation of pioglitazone has some effects on transcription related to oxidative stress, thus producing lower levels of protein carbonyls and HNE in the injured brain. However, we show here that pioglitazone's influence on mitochondrial bioenergetics is what drives neuroprotection and cognitive recovery after TBI.

Pioglitazone has shown therapeutic efficacy in Parkinson's disease. In a model of Parkinson's disease in rhesus monkeys, daily oral pioglitazone administration was shown to decrease inflammation and impart neuroprotection.<sup>74</sup> Recently, it was shown that a portion of this neuroprotection may be due to paraoxonase-2 activation, which in turn enhances mitochondrial function and reduces oxidative stress.<sup>72</sup> A more recent study highlights remarkable improvement in long-term cognition following TBI after chronic pioglitazone administration, starting 45 days post-injury.<sup>73</sup> Interestingly, this cognitive improvement did not coincide with an increase in PGC-1 $\alpha$  in animals treated with pioglitazone, which shows that pioglitazone may not be producing transcriptional changes but rather targeting mitoNEET to generate cognitive improvement. Importantly, this could be the mechanism of action as pioglitazone was given daily during behavioural testing and was therefore pharmacologically active.<sup>73</sup>

Although there was a decrease in maximal mitochondrial bioenergetics in the non-synaptic fraction at 48 h after experimental TBI and 18 h pioglitazone treatment, it is difficult to deduce the specific cell population this is a result of. This could potentially signify a decrease in oxidative phosphorylation in glia due to glycolytic shift. Further, it could also be related to assessment of dysfunctional mitochondria in the axon or neuronal soma during retrograde transport from the synapse, thereby promoting the usage of functional mitochondria in the synapse for mediation of neurotransmission. Indeed, following delayed pioglitazone treatment there are significant increases in State III mitochondrial bioenergetics (related to ATP production) for the synaptic fraction at both 48 h and 7 days after injury.

Remarkably, we observe lasting (over 5 months after injury) cognitive restoration with 18 h delayed pioglitazone treatment. By 165 days post-injury, all mice experience a drop in the time in target quadrant measure during the probe trial of MWM; it seems all mice are experiencing age-related cognitive decline by this time point. Interestingly, pioglitazone-treated sham group had higher target quadrant exploration compared to vehicle-treated sham group, suggesting pioglitazone can promote chronic neurobehavioural function, even in the absence of TBI. Additionally, pioglitazone-treated groups performed better in terms of platform crossing over time compared to vehicle-

treated groups, regardless of TBI. To corroborate this finding, the learning curves for the sham groups are not as steep at 165 days compared to 15 or 90 days post-injury. Nevertheless, we do observe consistent improvements imparted by pioglitazone treatment after TBI in the NOR task out to 150 days post-injury.

We acknowledge several limitations of this study. First, all experiments were performed in a model of CCI, an open skull injury. While this effectively models clinical TBI mechanisms, it would be interesting to evaluate pioglitazone and mitoNEET binding in a model of mild TBI, such as the closed head injury model, which also has documented mitochondrial dysfunction.<sup>26,40</sup> Further, we did not examine how neuroinflammation was modulated after pioglitazone treatment in these studies. Previous studies have found a therapeutic role for pioglitazone on the reduction of neuroinflammation after TBI<sup>12,74,75</sup> and interactions with PPAR- $\gamma$  may contribute to cognition recovery. It would have been useful to incorporate a PPAR- $\gamma$  inhibitor in the study design, such as T0070907,<sup>76</sup> although this was outside of the scope of the study. We do, however, show minimal therapeutic effect in mitoNEET null mice administered pioglitazone. These studies used both male and female wild-type and mitoNEET null animals (Supplementary Table 1), although these studies were not powered to detect sex differences. Future experiments should be performed to examine whether pioglitazone imparts therapeutic efficacy across sex.<sup>77,78</sup> There is a potential for sex-based differences in both the response to TBI and pioglitazone treatment, which is strong rationale for follow-up studies and should be considered when comparing these results to studies containing only male or female animals.

In future studies, we hope to use small molecules that bind to mitoNEET that could be used to pharmacologically treat TBI.<sup>79</sup> These novel mitoNEET ligands are constructed on the glitazone backbone by truncating the PPAR binding moiety,<sup>80</sup> which prevents activation of PPARs. Further, more studies need to be performed to understand the relationship between early mitophagy and initiation of pioglitazone treatment. Finally, we acknowledge the potential for therapeutic effects on multiple pathobiological processes, especially when translated to higher order animal models and humans. Recent research shows that pioglitazone plays a role in facilitating docosahexaenoic acid transport across the blood-brain barrier, which may in part contribute to better cognitive performance.<sup>81</sup>

In conclusion, delayed pioglitazone administration mitigates mitochondrial dysfunction, which produces ongoing neuroprotection and cognitive improvement. The therapeutic window of opportunity for pioglitazone seems to be biphasic, proving to produce bioenergetic restoration if administered immediately after injury<sup>12</sup> or delayed to after 12 h after injury, as observed in this study. Further, mitoNEET continues to prove to be a target of interest in treatment of neurodegenerative disease, namely TBI. Mounting evidence, including the study at hand, suggests that there may be a period after TBI where intrinsic mitochondrial machinery should not be manipulated. Endogenous mitochondrial processes, such as mitophagy, could be necessary early after injury (3–12 h) to eliminate dysfunctional mitochondria to either prevent apoptosis or restore adequate energy production through biogenesis pathways. Mitochondrial pharmaceuticals (mitoceuticals) still represent promising therapeutic approaches to eliminate ongoing secondary pathological consequences and restore neurological function, although therapeutic timing could be more important than previously regarded.

## Acknowledgements

We acknowledge Beverly Meachem at the Magnetic Resonance Imaging and Spectroscopy Center (MRISC), which is a service and consultation centre supporting basic and clinical research at the University of Kentucky, for assistance in MRI scanning. We would



like to thank Emily Brown for her help in visualization of the figures. Graphics created in Biorender.com

## Funding

This project was supported by BLR&D Department of Veterans Affairs Merit Award 1I01BX003405 (P.G.S.), by the Kentucky Spinal Cord and Head Injury Research Trust no. 15–14A (P.G.S.) and by NIH NINDS R01 NS112693-01A1 (P.G.S.). W.B.H. was supported by BLR&D Career Development Award Number IK2 BX004618 from the Department of Veterans Affairs and by a Kentucky Spinal Cord and Head Injury Research Trust fellowship. B.A.B. was supported by the National Institutes of Health [EY026584, AG058171]. The contents do not represent the views of the U.S. Department of Veterans Affairs or the United States Government. The content is solely the responsibility of the authors and does not necessarily represent the official views of the NIH.

The authors would like to thank the Redox Metabolism-Shared Resource Facility (RM-SRF) at the University of Kentucky for their technical assistance with slot blotting and acknowledge the NCI Cancer Center Support Grant (no. P30 CA177558). The work was also supported, in part, by grant 1 S10 OD023573-01 (MRISC) used to purchase the 7 T small animal scanner.

## Competing interests

The authors report no competing interests.

## Supplementary material

[Supplementary material](#) is available at *Brain* online.

## References

- Centers for Disease Control and Prevention. *Report to Congress on Traumatic Brain Injury in the United States: Epidemiology and Rehabilitation*. National Center for Injury Prevention and Control; Division of Unintentional Injury Prevention; 2015.
- Hubbard WB, Harwood CL, Geisler JG, Vekaria HJ, Sullivan PG. Mitochondrial uncoupling prodrug improves tissue sparing, cognitive outcome, and mitochondrial bioenergetics after traumatic brain injury in male mice. *J Neurosci Res*. 2018;96(10):1677–1688.
- Pandya JD, Pauly JR, Nukala VN, et al. Post-injury administration of mitochondrial uncouplers increases tissue sparing and improves behavioral outcome following traumatic brain injury in rodents. *J Neurotrauma*. 2007;24(5):798–811.
- Readnower RD, Pandya JD, McEwen ML, Pauly JR, Springer JE, Sullivan PG. Post-injury administration of the mitochondrial permeability transition pore inhibitor, NIM811, is neuroprotective and improves cognition after traumatic brain injury in rats. *J Neurotrauma*. 2011;28(9):1845–1853.
- Scheff SW, Sullivan PG. Cyclosporin A significantly ameliorates cortical damage following experimental traumatic brain injury in rodents. *J Neurotrauma*. 1999;16(9):783–792.
- Sullivan PG, Sebastian AH, Hall ED. Therapeutic window analysis of the neuroprotective effects of cyclosporine A after traumatic brain injury. *J Neurotrauma*. 2011;28(2):311–318.
- Hubbard WB, Davis LM, Sullivan PG. Mitochondrial damage in traumatic CNS injury. In: Fujikawa DG, ed. *Acute neuronal injury: The role of excitotoxic programmed cell death mechanisms*. Springer International Publishing; 2018: 63–81.
- Karlsson M, Yang Z, Chawla S, et al. Evaluation of diffusion tensor imaging and fluid based biomarkers in a large animal trial of cyclosporine in focal traumatic brain injury. *J Neurotrauma*. 2021;38(13):1870–1878.
- Pandya JD, Readnower RD, Patel SP, et al. N-acetylcysteine amide confers neuroprotection, improves bioenergetics and behavioral outcome following TBI. *Exp Neurol*. 2014;257:106–113.
- Vekaria HJ, Hubbard WB, Scholpa NE, et al. Formoterol, a beta2-adrenoreceptor agonist, induces mitochondrial biogenesis and promotes cognitive recovery after traumatic brain injury. *Neurobiol Dis*. 2020;140:104866.
- Yonutas HM, Hubbard WB, Pandya JD, Vekaria HJ, Geldenhuys WJ, Sullivan PG. Bioenergetic restoration and neuroprotection after therapeutic targeting of mitoNEET: New mechanism of pioglitazone following traumatic brain injury. *Exp Neurol*. 2020; 327:113243.
- Sauerbeck A, Gao J, Readnower R, et al. Pioglitazone attenuates mitochondrial dysfunction, cognitive impairment, cortical tissue loss, and inflammation following traumatic brain injury. *Exp Neurol*. 2011;227(1):128–135.
- Smith U. Pioglitazone: Mechanism of action. *Int J Clin Pract Suppl*. 2001;(121):13–18.
- Qi L, Jacob A, Wang P, Wu R. Peroxisome proliferator activated receptor-gamma and traumatic brain injury. *Int J Clin Exp Med*. 2010;3(4):283–292.
- Kiaei M. Peroxisome proliferator-activated receptor-gamma in amyotrophic lateral sclerosis and Huntington's disease. *PPAR Res*. 2008;2008:418765.
- Villapol S. Roles of peroxisome proliferator-activated receptor gamma on brain and peripheral inflammation. *Cell Mol Neurobiol*. 2018;38(1):121–132.
- Semple BD, Noble-Haeusslein LJ. Broad-spectrum neuroprotection against traumatic brain injury by agonism of peroxisome proliferator-activated receptors. *Exp Neurol*. 2011;229(2): 195–197.
- Thal SC, Heinemann M, Luh C, Pieter D, Werner C, Engelhard K. Pioglitazone reduces secondary brain damage after experimental brain trauma by PPAR-gamma-independent mechanisms. *J Neurotrauma*. 2011;28(6):983–993.
- Paddock ML, Wiley SE, Axelrod HL, et al. MitoNEET is a uniquely folded 2Fe 2S outer mitochondrial membrane protein stabilized by pioglitazone. *Proc Natl Acad Sci U S A*. 2007;104(36):14342–14347.
- Bieganski RM, Yarmush ML. Novel ligands that target the mitochondrial membrane protein mitoNEET. *J Mol Graph Model*. 2011; 29(7):965–973.
- Rabchevsky AG, Patel SP, Sullivan PG. Targeting mitoNEET with pioglitazone for therapeutic neuroprotection after spinal cord injury. *Neural Regen Res*. Nov 2017;12(11):1807–1808.
- Kusminski CM, Holland WL, Sun K, et al. MitoNEET-driven alterations in adipocyte mitochondrial activity reveal a crucial adaptive process that preserves insulin sensitivity in obesity. *Nat Med*. 2012;18(10):1539–1549.
- Golinelli-Cohen M-P, Lescop E, Mons C, et al. Redox control of the human iron-sulfur repair protein MitoNEET activity via its iron-sulfur cluster. *J Biol Chem*. 2016;291(14):7583–7593.
- Geldenhuys WJ, Benkovic SA, Lin L, et al. MitoNEET (CISD1) knockout mice show signs of striatal mitochondrial dysfunction and a Parkinson's disease phenotype. *ACS Chem Neurosci*. 2017;8(12):2759–2765.
- Wiley SE, Murphy AN, Ross SA, van der Geer P, Dixon JE. MitoNEET is an iron-containing outer mitochondrial membrane protein that regulates oxidative capacity. *Proc Natl Acad Sci U S A*. 2007;104(13):5318–5323.
- Hubbard WB, Joseph B, Spry M, Vekaria HJ, Saatman KE, Sullivan PG. Acute mitochondrial impairment underlies prolonged cellular dysfunction after repeated mild traumatic brain injuries. *J Neurotrauma*. 2019;36(8):1252–1263.

27. Hubbard WB, Harwood CL, Prajapati P, Springer JE, Saatman KE, Sullivan PG. Fractionated mitochondrial magnetic separation for isolation of synaptic mitochondria from brain tissue. *Sci Rep*. 2019;9(1):9656.
28. Pischiutta F, Micotti E, Hay JR, et al. Single severe traumatic brain injury produces progressive pathology with ongoing contralateral white matter damage one year after injury. *Exp Neurol*. 2018;300:167–178.
29. Jenkinson M, Pechaud M, Smith S. BET2: MR-based estimation of brain skull and scalp surfaces. In: *International Conference on Human Brain Mapping*. 2005.
30. Avants BB, Tustison NJ, Song G, Cook PA, Klein A, Gee JC. A reproducible evaluation of ANTs similarity metric performance in brain image registration. *Neuroimage*. 2011;54(3):2033–2044.
31. Avants BB, Epstein CL, Grossman M, Gee JC. Symmetric diffeomorphic image registration with cross-correlation: Evaluating automated labeling of elderly and neurodegenerative brain. *Med Image Anal*. 2008;12(1):26–41.
32. Jenkinson M, Smith S. A global optimisation method for robust affine registration of brain images. *Med Image Anal*. 2001;5(2):143–156.
33. Jenkinson M, Bannister P, Brady M, Smith S. Improved optimization for the robust and accurate linear registration and motion correction of brain images. *Neuroimage*. 2002;17(2):825–841.
34. Geldenhuys WJ, Long TE, Saralkar P, et al. Crystal structure of the mitochondrial protein mitoNEET bound to a benze-sulfo-nide ligand. *Commun Chem*. 2019;2:77.
35. Pandya JD, Pauly JR, Sullivan PG. The optimal dosage and window of opportunity to maintain mitochondrial homeostasis following traumatic brain injury using the uncoupler FCCP. *Exp Neurol*. 2009;218(2):381–389.
36. Mohamadpour M, Whitney K, Bergold PJ. The importance of therapeutic time window in the treatment of traumatic brain injury. *Front Neurosci*. 2019;13:07.
37. Diaz-Arrastia R, Kochanek PM, Bergold P, et al. Pharmacotherapy of traumatic brain injury: State of the science and the road forward: Report of the Department of Defense Neurotrauma Pharmacology Workgroup. *J Neurotrauma*. 2014;31(2):135–158.
38. Hill RL, Singh IN, Wang JA, Hall ED. Time courses of post-injury mitochondrial oxidative damage and respiratory dysfunction and neuronal cytoskeletal degradation in a rat model of focal traumatic brain injury. *Neurochem Int*. 2017;111:45–56.
39. Kulbe JR, Hill RL, Singh IN, Wang JA, Hall ED. Synaptic mitochondria sustain more damage than non-synaptic mitochondria after traumatic brain injury and are protected by cyclosporine A. *J Neurotrauma*. 2017;34(7):1291–1301.
40. Lyons DN, Vekaria H, Macheda T, et al. A mild traumatic brain injury in mice produces lasting deficits in brain metabolism. *J Neurotrauma*. 2018;35(20):2435–2447.
41. Jonas E. Regulation of synaptic transmission by mitochondrial ion channels. *J Bioenerg Biomembr*. 2004;36(4):357–361.
42. Tucker LB, Velosky AG, McCabe JT. Applications of the Morris water maze in translational traumatic brain injury research. *Neurosci Biobehav Rev*. 2018;88:187–200.
43. Brody DL, Holtzman DM. Morris water maze search strategy analysis in PDAPP mice before and after experimental traumatic brain injury. *Exp Neurol*. 2006;197(2):330–340.
44. Pleasant JM, Carlson SW, Mao H, Scheff SW, Yang KH, Saatman KE. Rate of neurodegeneration in the mouse controlled cortical impact model is influenced by impactor tip shape: Implications for mechanistic and therapeutic studies. *J Neurotrauma*. 2011;28(11):2245–2262.
45. Yang T, Soodvilai S. Renal and vascular mechanisms of thiazolidinedione-induced fluid retention. *PPAR Res*. 2008;2008:943614.
46. Nesto RW, Bell D, Bonow RO, et al. Thiazolidinedione use, fluid retention, and congestive heart failure: A consensus statement from the American Heart Association and American Diabetes Association. *Diabetes Care*. 2004;27(1):256–263.
47. Unterberg AW, Stover J, Kress B, Kiening KL. Edema and brain trauma. *Neuroscience*. 2004;129(4):1021–1029.
48. Carlson SW, Saatman KE. Central infusion of insulin-like growth factor-1 increases hippocampal neurogenesis and improves neurobehavioral function after traumatic brain injury. *J Neurotrauma*. 2018;35(13):1467–1480.
49. Yi J-H, Park S-W, Brooks N, Lang BT, Vemuganti R. PPARgamma agonist rosiglitazone is neuroprotective after traumatic brain injury via anti-inflammatory and anti-oxidative mechanisms. *Brain Res*. 2008;1244:164–172.
50. Besson VC, Chen XR, Plotkine M, Marchand-Verrecchia C. Fenofibrate, a peroxisome proliferator-activated receptor alpha agonist, exerts neuroprotective effects in traumatic brain injury. *Neurosci Lett*. 2005;388(1):7–12.
51. Chen XR, Besson VC, Palmier B, Garcia Y, Plotkine M, Marchand-Leroux C. Neurological recovery-promoting, anti-inflammatory, and anti-oxidative effects afforded by fenofibrate, a PPAR alpha agonist, in traumatic brain injury. *J Neurotrauma*. 2007;24(7):1119–1131.
52. Hyong A, Jadhav V, Lee S, et al. Rosiglitazone, a PPAR gamma agonist, attenuates inflammation after surgical brain injury in rodents. *Brain Res*. 2008;1215:218–224.
53. Pilipovic K, Zupan Z, Dolenec P, Mrcic-Pelcic J, Zupan G. A single dose of PPARgamma agonist pioglitazone reduces cortical oxidative damage and microglial reaction following lateral fluid percussion brain injury in rats. *Prog Neuro-Psychopharmacol Biol Psychiatry*. 2015;59:8–20.
54. Corona JC, Duchon MR. PPAR $\gamma$  as a therapeutic target to rescue mitochondrial function in neurological disease. *Free Radical Biol Med*. 2016;100:153–163.
55. Zuris JA, Harir Y, Conlan AR, et al. Facile transfer of [2Fe-2S] clusters from the diabetes drug target mitoNEET to an apo-acceptor protein. *Proc Natl Acad Sci U S A*. 2011;108(32):13047–13052.
56. Andersen BJ, Marmarou A. Post-traumatic selective stimulation of glycolysis. *Brain Res*. 1992;585(1-2):184–189.
57. Bergsneider M, Hovda DA, Shalmon E, et al. Cerebral hyperglycolysis following severe traumatic brain injury in humans: A positron emission tomography study. *J Neurosurg*. 1997;86(2):241–251.
58. Carpenter KLH, Jalloh I, Hutchinson PJ. Glycolysis and the significance of lactate in traumatic brain injury. *Front Neurosci*. 2015;9:112.
59. Sullivan PG, Rabchevsky AG, Hicks RR, Gibson TR, Fletcher-Turner A, Scheff SW. Dose-response curve and optimal dosing regimen of cyclosporin A after traumatic brain injury in rats. *Neuroscience*. 2000;101(2):289–295.
60. Kenny EM, Fidan E, Yang Q, et al. Ferroptosis contributes to neuronal death and functional outcome after traumatic brain injury. *Crit Care Med*. 2019;47(3):410–418.
61. Daglas M, Adlard PA. The involvement of iron in traumatic brain injury and neurodegenerative disease. *Front Neurosci*. 2018;12:981.
62. Martinez-Vicente M. Neuronal mitophagy in neurodegenerative diseases. *Front Mol Neurosci*. 2017;10:64.
63. Sedlackova L, Korolchuk VI. Mitochondrial quality control as a key determinant of cell survival. *Biochim Biophys Acta Mol Cell Res*. 2019;1866(4):575–587.

64. Kusminski CM, Park J, Scherer PE. MitoNEET-mediated effects on browning of white adipose tissue. *Nat Commun.* 2014;5(1):3962.
65. Vernay A, Marchetti A, Sabra A, et al. MitoNEET-dependent formation of intermitochondrial junctions. *Proc Natl Acad Sci U S A.* 2017;114(31):8277–8282.
66. Chao H, Lin C, Zuo Q, et al. Cardiolipin-dependent mitophagy guides outcome after traumatic brain injury. *J Neurosci.* 2019;39(10):1930–1943.
67. Lamade AM, Anthonyamuthu TS, Hier ZE, Gao Y, Kagan VE, Bayir H. Mitochondrial damage & lipid signaling in traumatic brain injury. *Exp Neurol.* 2020;329:113307.
68. Lazarou M, Narendra DP, Jin SM, Tekle E, Banerjee S, Youle RJ. PINK1 drives Parkin self-association and HECT-like E3 activity upstream of mitochondrial binding. *J Cell Biol.* 2013;200(2):163–172.
69. Ansari MA, Roberts KN, Scheff SW. Oxidative stress and modification of synaptic proteins in hippocampus after traumatic brain injury. *Free Radic Biol Med.* 2008;45(4):443–452.
70. Hall ED. The contributing role of lipid peroxidation and protein oxidation in the course of CNS injury neurodegeneration and neuroprotection: An overview. In: Kobeissy FH, ed. *Brain neurotrauma: Molecular, neuropsychological, and rehabilitation aspects.* CRC Press/Taylor & Francis; 2015.
71. Swanson CR, Joers V, Bondarenko V, et al. The PPAR-gamma agonist pioglitazone modulates inflammation and induces neuroprotection in parkinsonian monkeys. *J Neuroinflamm.* 2011;8:91.
72. Blackburn JK, Curry DW, Thomsen AN, Roth RH, Elsworth JD. Pioglitazone activates paraoxonase-2 in the brain: A novel neuroprotective mechanism. *Exp Neurol.* 2020;327:113234.
73. McGuire JL, Correll EA, Lowery AC, et al. Pioglitazone improves working memory performance when administered in chronic TBI. *Neurobiol Dis.* 2019;132:104611.
74. Liu M, Bachstetter AD, Cass WA, Lifshitz J, Bing G. Pioglitazone attenuates neuroinflammation and promotes dopaminergic neuronal survival in the nigrostriatal system of rats after diffuse brain injury. *J Neurotrauma.* 2017;34(2):414–422.
75. Das M, Mayilsamy K, Tang X, et al. Pioglitazone treatment prior to transplantation improves the efficacy of human mesenchymal stem cells after traumatic brain injury in rats. *Sci Rep.* 2019;9(1):13646.
76. Deng Y, Jiang X, Deng X, et al. Pioglitazone ameliorates neuronal damage after traumatic brain injury via the PPAR $\gamma$ /NF- $\kappa$ B/IL-6 signaling pathway. *Genes Dis.* 2020;7(2):253–265.
77. Gupte R, Brooks W, Vukas R, Pierce J, Harris J. Sex differences in traumatic brain injury: What we know and what we should know. *J Neurotrauma.* 2019;36(22):3063–3091.
78. Arambula SE, Reindl EL, El Demerdash N, McCarthy MM, Robertson CL. Sex differences in pediatric traumatic brain injury. *Exp Neurol.* 2019;317:168–179.
79. Geldenhuys WJ, Yonutas HM, Morris DL, Sullivan PG, Darvesh AS, Leeper TC. Identification of small molecules that bind to the mitochondrial protein mitoNEET. *Bioorg Med Chem Lett.* 2016;26(21):5350–5353.
80. Tamir S, Paddock ML, Darash-Yahana-Baram M, et al. Structure-function analysis of NEET proteins uncovers their role as key regulators of iron and ROS homeostasis in health and disease. *Biochim Biophys Acta.* 2015;1853(6):1294–1315.
81. Low YL, Jin L, Morris ER, Pan Y, Nicolazzo JA. Pioglitazone increases blood-brain barrier expression of fatty acid-binding protein 5 and docosahexaenoic acid trafficking into the brain. *Mol Pharm.* 2020;17(3):873–884.